A Late Ordovician Conodont Fauna from the Lower Limestone Member of the Benjamin Limestone in Central Tasmania, and Revision of *Tasmanognathus careyi* Burrett, 1979

Y.Y. Zhen[1], C.F. Burrett[2], I.G. Percival[3] and B.Y. Lin[4]

[1]Australian Museum, 6 College Street, Sydney, N.S.W. 2010, Australia (yongyi.zhen@austmus.gov.au);
[2]School of Earth Sciences, University of Tasmania, GPO Box 79, Hobart, Tasmania 7001, Australia (cliveburrett@gmail.com);
[3]Geological Survey of New South Wales, 947-953 Londonderry Road, Londonderry, N.S.W. 2753, Australia (ian.percival@industry.nsw.gov.au);
[4]Institute of Geology, Chinese Academy of Geological Sciences, Beijing, China, 100037.

Zhen, Y.Y., Burrett, C.F., Percival, I.G. and Lin, B.Y. (2010). A Late Ordovician conodont fauna from the Lower Limestone Member of the Benjamin Limestone in central Tasmania, and revision of *Tasmanognathus careyi* Burrett, 1979. *Proceedings of the Linnean Society of New South Wales* **131**, 43-72.

Ten conodont species, including *Aphelognathus*? sp., *Belodina compressa*, *Chirognathus tricostatus* sp. nov., *Drepanodus* sp., gen. et sp. indet., *Panderodus gracilis*, *Protopanderodus*? *nogamii*, *Phragmodus undatus*, *Tasmanognathus careyi* and *T.* sp. cf. *T. careyi* are documented from the Lower Limestone Member of the Benjamin Limestone, Gordon Group, exposed in the Florentine Valley and Everlasting Hills region of central Tasmania. For the first time since its establishment three decades ago, the type species of *Tasmanognathus, T. careyi,* is revised with recognition of a septimembrate apparatus including makellate M, alate Sa, digyrate Sb, bipennate Sc, tertiopedate Sd, carminate Pa, and Pb (angulate Pb1 and pastinate Pb2) elements. Co-occurrence of *Phragmodus undatus* and *Belodina compressa* in the fauna indicates a latest Sandbian to earliest Katian (*Phragmodus undatus* conodont Zone) age for the Lower Limestone Member of the Benjamin Limestone. All species previously attributed to *Tasmanognathus* are briefly reviewed, and the distribution of the genus is shown to be more widespread than hitherto recognised (in New South Wales, North China, Tarim Basin, South Korea and northeast Russia), with a probable occurrence in North American Midcontinental faunas.

Manuscript received 16 September 2009, accepted for publication 26 May 2010.

KEYWORDS: Benjamin Limestone, biogeography, biostratigraphy, conodonts, Late Ordovician, Tasmania, *Tasmanognathus*.

INTRODUCTION

Ordovician conodont faunas of Tasmania are relatively poorly known in comparison to those from the mainland of Eastern Australia. Only three papers – Burrett (1979), Burrett et al. (1983) and Cantrill and Burrett (2004) – have dealt systematically with a small number of species. The present contribution, which describes the comparatively diverse fauna from the lower part of the Benjamin Limestone, is the first part of a revision of all known conodonts from Tasmania. This project aims to provide a firm basis for conodont-based correlations of the carbonate-dominated Gordon Group with limestones along the Delamerian continental margin in New South Wales, with strata in offshore island arc settings in central N.S.W. (Macquarie Arc), and with isolated limestone pods in the New England Orogen in northeastern N.S.W. and central Queensland.

Given the rarity of graptolites in the predominantly shallow-water platformal succession forming the Delamerian margin succession, and the sparsely documented occurrences of conodonts,

biostratigraphical zonation in Ordovician rocks of Tasmania is currently largely reliant on shelly macrofossils. Banks and Burrett (1980) established a series of twenty successive faunas (designated OT assemblages 1-20), one of which (OT 12) was defined by the occurrence of several conodont species including *Tasmanognathus careyi*, *Chirognathus monodactyla*, *Erismodus gracilis* and *Plectodina aculeata* in the basal Benjamin Limestone. This fauna (based at the time on unpublished studies by Burrett, with no species illustrated or described in the 1980 paper) is revised here. Our study has not identified the last two named species, and has recognised a new species of *Chirognathus* in place of *C. monodactyla*. Burrett (in Webby et al. 1981, p.12) summarised the occurrences of conodonts in the Tasmanian Ordovician succession. He noted the first appearance of the biostratigraphically important species *Phragmodus undatus* in strata immediately above the Lords Siltstone Member in the middle of the Benjamin Limestone; however, our reassessment of the fauna has identified the presence of this species in the underlying lower part of the Benjamin Limestone. Laurie (1991) defined an alternate series of 20 faunal assemblages based on Tasmanian brachiopods, ranging in age from Early Ordovician (Tremadocian) to earliest Silurian. Where possible, these brachiopod faunas were tied in to conodont occurrences, mainly derived from Burrett's (1978) unpublished thesis studies.

A biogeographically significant component of the Tasmanian conodont fauna is *Tasmanognathus* Burrett, 1979, which was first identified from the Lower Limestone Member of the Benjamin Limestone exposed in the Florentine Valley and Everlasting Hills region of central Tasmania (Fig. 1). This genus has subsequently been widely recognized as occurring in rocks of early Late Ordovician (Sandbian) age in eastern Australia and China. Low yields (averaging two specimens per kg) of conodonts from the Gordon Group carbonates collected and processed by Burrett (1978) resulted in *Tasmanognathus* being imperfectly defined. Thirty years after its initial documentation, revision of the type species, *T. careyi* Burrett, 1979 has become urgently needed in order to better understand its multielement apparatus, phylogenetic relationship and precise stratigraphic range in the type area. The purpose of this paper is to describe the conodont fauna from the middle part of the Gordon Group in the Settlement Road section of the Florentine Valley area, equivalent to the level yielding *Tasmanognathus*, based on five recently collected bulk samples of limestone totalling 49.5 kg that on dissolution in acetic acid have yielded an average of six elements per kg. These additional collections are supplemented by re-examination of Burrett's original material including types and topotypes of *T. careyi*, and for the first time all the accompanying conodont fauna is documented by description and/or illustration, including *Aphelognathus*? sp., *Belodina compressa* (Branson and Mehl, 1933), *Chirognathus tricostatus* sp. nov., *Drepanodus* sp., *Panderodus gracilis* (Branson and Mehl, 1933), *Protopanderodus? nogamii* (Lee, 1975), *Phragmodus undatus* Branson and Mehl, 1933, and gen. et sp. indet.

REGIONAL GEOLOGIC AND BIOSTRATIGRAPHIC SETTING

Platform sedimentary rocks of the Early Palaeozoic Wurawina Supergroup, that are widespread in the western half of Tasmania, consist of the Late Cambrian – Early Ordovician Denison Group (mainly siliciclastics), conformably overlain by the Gordon Group (predominantly carbonates of Early to Late Ordovician age), in turn conformably or disconformably overlain by the Hirnantian (latest Ordovician) to mid-Devonian Eldon Group, which consists mainly of siliciclastics (Burrett *et al.* 1984; Laurie 1991). The Gordon Group attains a thickness of 2100m of carbonates and minor siltstones in its redefined type section in the Florentine Valley where it is divided into three limestone formations. The uppermost of these, the Benjamin Limestone, is divided into two limestone members (Upper and Lower) separated by a thin but regionally extensive, macrofossiliferous siltstone member (Lords Siltstone Member). The Benjamin Limestone predominantly consists of interbedded microcrystalline peritidal dolomitic micrite, dolostone and calcarenite with a maximum thickness of about 1200m. Some 400 conodont samples were initially collected over a 5m interval by Burrett (1978) from the various localities of the Gordon Group, but many of these samples were barren or had a very low yield, due to the peritidal to shallow subtidal depositional setting and high rate of sedimentation in the tropical shelf environments. Continuous efforts in the last 30 years by post-graduate students and academic staff of the University of Tasmania have accumulated significant amounts of conodont material for the age determination and biostratigraphic analysis of the Gordon Group (Burrett 1979; Burrett *et al.* 1983, 1984; Cantrill and Burrett 2004).

Carbonates that are coeval with the Lower Limestone Member of the Benjamin Limestone occur in many sections in northern, western and southern

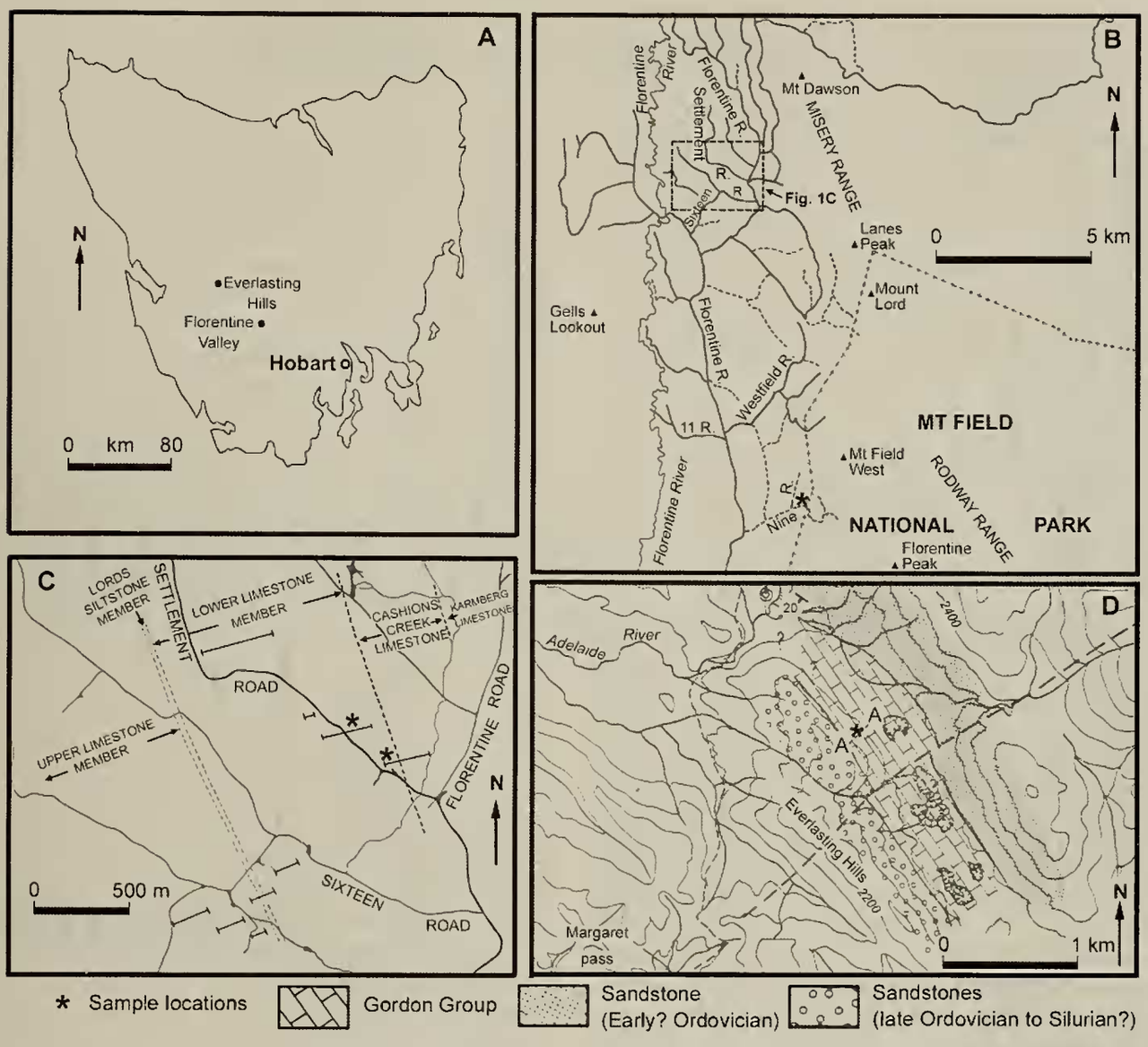

Figure 1. Maps showing the studied areas in central Tasmania and sample locations. A, Map of Tasmania showing the locations of Florentine Valley and Everlasting Hills (from Burrett 1978, 1979); B, Map showing the Florentine Valley area and sample location of the Nine Road Section (modified from Laurie 1991); C, Map showing the Settlement Road Section of the Florentine Valley and sample locations (modified from Laurie 1991); D, Map showing Everlasting Hills area and sample location (from Burrett 1978).

Tasmania, but the *Tasmanognathus careyi* fauna has only been definitely found in the Florentine Valley and in the Everlasting Hills. The Florentine Valley sections (Figs 1 and 2) are found in the eastern side of a mid-Devonian synclinorial structure. This area was first mapped geologically by Corbett and Banks (1974) and because of its completeness, has subsequently been the focus of numerous palaeontological and sedimentological studies. However, active timber logging in this area has meant that some sections are now inaccessible, having been replanted with dense, almost impenetrable, forest.

The Everlasting Hills section (Fig.1D) was discovered in remote and moderately dense to thick vegetation and mapped by Ian McKendrick and Clive Burrett in 1975 (Fig.1D). This doline and cave-rich area has since been included in the South West Tasmania World Heritage wilderness area, and has undergone extensive regrowth so that it is now extremely difficult to access. The palaeotropical limestones in the Everlasting Hills are identical to those in the Lower Limestone Member of the Benjamin Limestone in the Florentine Valley, and consist of 3-6m thick Punctuated Aggradational Cycles (Goodwin and Anderson 1985) of mainly dolomitised, intertidal micrites with tidal channels and top beds containing a lower intertidal to high subtidal macrofauna. Somewhat deeper water, coeval carbonates (the Ugbrook Formation) occur in

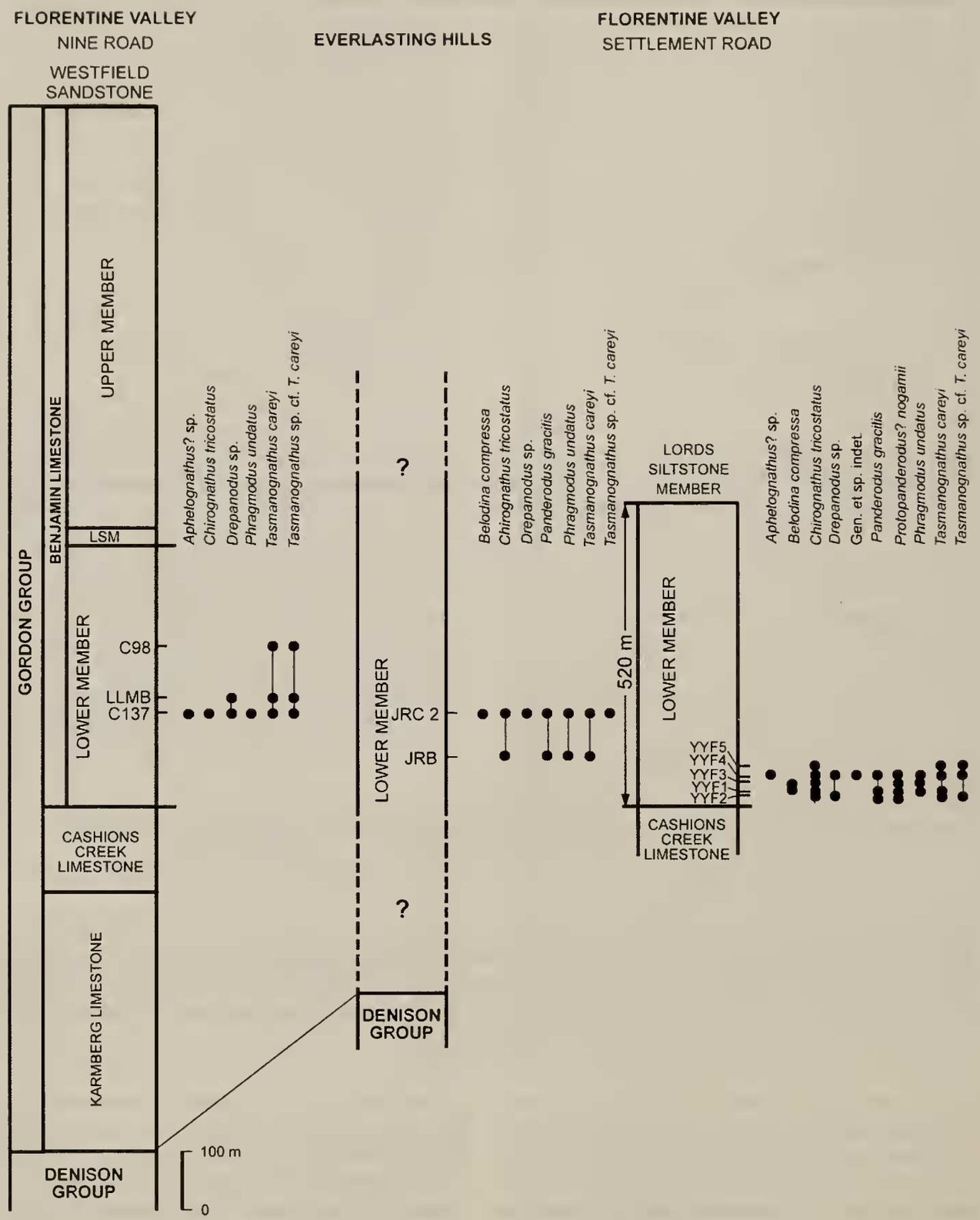

Figure 2. Three stratigraphic sections showing the sample horizons and ranges of the conodont species in the Lower Limestone Member of the Benjamin Limestone, Gordon Group, in central Tasmania.

northern and western Tasmania (Burrett et al. 1989) but these lack *Tasmanognathus*. This suggests that *Tasmanognathus* was mainly restricted to peritidal tropical environments in the Late Ordovician.

The *Tasmanognathus* fauna is associated with a strongly endemic macrofauna in the lower and middle parts of the Lower Limestone Member, Benjamin Limestone, including the brachiopods *Lepidomena* Laurie, 1991, *Tasmanorthis* Laurie, 1991 and the nautiloids *Gorbyoceras settlementense* Stait and Flower, 1985, *Paramadiganella* Stait, 1984 and *Tasmanoceras zeehanense* Teichert and Glenister, 1952 (Laurie 1991; Stait 1988). *Tasmanognathus careyi* is found in two of the twenty Ordovician brachiopod assemblages (or biozones) recognised by Laurie (1991); the *Tasmanorthis calveri* and the younger *Tasmanorthis costata* assemblages.

AGE AND CORRELATION OF THE FAUNA

In the conodont fauna associated with *Tasmanognathus careyi* from the Lower Limestone Member of the Benjamin Limestone in central Tasmania, occurrence of *Phragmodus undatus* and *Belodina compressa* is crucial for age determination and regional correlation, as both species are cosmopolitan and age diagnostic. The former had a relatively long stratigraphic range, extending from the base of the *Ph. undatus* Zone (in the upper Sandbian) to the top of the Katian, and the latter first occurs at the base of the *B. compressa* Zone and extends to the base of the *B. confluens* Zone (Sweet 1988). Co-occurrence of these two species and absence of any diagnostic species of either the *B. confluens* or *P. tenuis* zones indicates a latest Sandbian to earliest Katian age (*Phragmodus undatus* Zone) for this Tasmanian fauna.

Chirognathus is also morphologically distinctive with the two previously-reported species (*Chirognathus duodactylus* Branson and Mehl, 1933 and *Chirognathus cliefdenensis* Zhen and Webby, 1995) restricted to the upper Sandbian-Katian interval (Sweet 1982; Zhen & Webby 1995). The new species from Tasmania described herein is morphologically similar to the type species of the genus, *C. duodactylus* Branson and Mehl, 1933. This species with a well-known multi-element apparatus is widely distributed in Sandbian strata of the North American Mid-continent ranging from the *Pygodus anserinus* Zone to the *Phragmodus undatus* Zone (Sweet in Ziegler 1991). The second species, *Chirognathus cliefdenensis* Zhen and Webby, 1995, occurs in a stratigraphically slightly younger interval in central New South Wales, where it is recorded from the upper Fossil Hill Limestone to the lower Vandon Limestone (early Katian) of the Cliefden Caves Limestone Subgroup (Zhen and Webby 1995), from the Downderry Limestone Member (late Katian) of the Ballingoole Limestone of the Bowan Park Limestone Subgroup (Zhen et al. 1999), and from allochthonous limestones of Katian age emplaced in the Silurian Barnby Hills Shale (Zhen et al. 2003a).

The Lower Limestone Member of the Benjamin Limestone exposed in the Everlasting Hills and Florentine Valley areas in central Tasmania is the type stratum of *Tasmanognathus careyi* Burrett, 1979. Since the initial documentation of this species, at least ten additional species from lower Sandbian to upper Katian strata predominantly of North China and eastern Australia have been accommodated in *Tasmanognathus* (see Systematic section for further discussion). The origin and phylogenetic relationships of *Tasmanognathus* remain uncertain as most of these species were poorly documented and need to be revised. Reassessment of *T. careyi* herein suggests that *Tasmanognathus* may be closely related to so-called "Ordovician ozarkodinides" (Sweet 1988, p. 91-92), an informal group including forms like "*Plectodina*", *Aphelognathus* and *Yaoxianognathus*. Based on similarities of their general morphology and apparatus construction, *Tasmanognathus*, as a sister group, seems closely related to *Yaoxianognathus*. *Tasmanognathus* is potentially the direct ancestor of the latter, which was mainly restricted to eastern Gondwana and peri-Gondwanan terranes during the Late Ordovician (Katian). Strong biogeographic similarities (including *Tasmanognathus*) between the North China Terrane (or block) and eastern Australia were part of the evidence used by Burrett et al. (1990) to suggest that these blocks were contiguous or closely proximal during the Ordovician.

Tasmanognathus was widely reported from the Sandbian in North China with recognition of three biozones based on the inferred lineage of *Tasmanognathus* species (An and Zheng 1990; Lin and Qiu 1990), from the oldest *T. sishuiensis* Zhang in An et al., 1983 from the upper Fengfeng Formation (lower Sandbian), to *T. shichuanheensis* An in An et al., 1985 from the middle-lower part of the Yaoxian Formation (upper Sandbian), and then to the youngest *T. multidentatus* An in An and Zheng, 1990 (the latter is a *nomem nudum*, equivalent to *T. borealis* An in An et al. 1985; see Systematic Section for further discussion) from the upper part of the Yaoxian Formation (upper Sandbian-lower Katian). An and Zheng (1990, p. 95, text-fig. 9) illustrated the morphological changes from *T. sishuiensis* with a

robust cusp and small, widely spaced denticles on the processes of the S elements, to *T. multidentatus* with a small, indistinct cusp in the Pa element and closer spaced denticles of variable sizes on the processes of the S elements. Importantly, similar morphological changes have also been observed between the two species of *Tasmanognathus* recognized in the Lower Limestone Member of the Benjamin Limestone in central Tasmania. A species described herein as *T.* sp. cf. *T. careyi* that bears a prominent cusp in the Pa element and small, widely spaced denticles on the processes of the S and Pb elements is more comparable with *T. shichuanheensis* from the middle-lower part of the Yaoxian Formation, whereas *T. careyi* with a small or indistinct cusp in the Pa element and long, closely spaced denticles on the processes of the S elements is closer to *T. multidentatus* from the upper part of the Yaoxian Formation. *T. careyi* was also reported from the middle part of the Yaoxian Formation in association with *T. shichuanheensis* and *Belodina compressa* in Bed 3, about 44 m below the first occurrence of *T. multidentatus* (An and Zheng 1990, p. 86-87), although An's identification cannot be confirmed without re-examination of the original material (An et al. 1985) and further investigations.

Occurrence of *Taoqupognathus blandus* at the top of the Yaoxian Formation in the Taoqupo Section of Yaoxian County (formerly Yaoxian; An and Zheng 1990) suggests that the Yaoxian Formation may well extend to the lower Katian. Therefore, the morphological characters shown by the two species of *Tasmanognathus* from the Lower Limestone Member of the Benjamin Limestone support a correlation between this limestone unit in central Tasmania, and the middle part of the Yaoxian Formation in North China (with the possible occurrence of *T. careyi*), which An and Zheng (1990, p. 92, table 2) correlated with the *C. wilsoni* graptolite Zone (late Sandbian).

An and Zheng (1990, p.115) suggested that the Llandoverian conodonts illustrated by Lee (1982) from the Hoedongri Formation in the Taebaeksan Basin, Kangweon-Do of South Korea were comparable with the *Tasmanognathus sishuiensis* assemblage from the upper Fengfeng Formation of North China. In fact, in their revision of Lee's original identifications (An and Zheng 1990, table 5, pp. 118-119), they believed what Lee (1982) illustrated as *Pterospathodus celloni* (Walliser) should belong to *Tasmanognathus sishuiensis*, and considered that the Hoedongri Formation should be correlated with the Baduo Formation or the upper part of the Fengfeng Formation (Sandbian) of North China.

MATERIAL AND SAMPLING LOCALITIES

The current study is based on 683 identifiable specimens from 10 samples (See Table 1). Of these,

Table 1. Distribution of conodont species in the samples studied.

species	JRC 2	JRB	LLMB	C137	C98	YYF1	YYF2	YYF3	YYF4	YYF5	Total
Aphelognathus? sp.				2					2		4
Belodina compressa	9							1			10
Chirognathus tricostatus sp. nov.	36	6		12		2	1	1	5	8	71
Drepanodus sp.	20		1	2		1	1		2		27
Gen. et sp. indet.									3		3
Panderodus gracilis	41	2	4				3		2		52
Protopanderodus? *nogamii*						4	44	3	18		69
Phragmodus undatus	25	2		6		1		31	51		116
Tasmanognathus careyi	156	5	20	26	26	7	23		23	11	297
Tasmanognathus sp. cf. *T. careyi*	3					8	7		14	2	34
Total	290	15	25	48	26	23	79	36	120	21	683

378 specimens are Burrett's (1979) original material including types of *Tasmanognathus careyi* recovered from five samples collected from the Florentine Valley and Everlasting Hills sections (see Burrett 1979, p. 32, fig. 1 for sample locations and their stratigraphic horizons within the Lower Member of the Benjamin Limestone). Samples LLMB, C137 and C98 were collected from the Lower Limestone Member of the Benjamin Limestone exposed along the Nine Road (Fig. 1B). The Lower Limestone Member of the Benjamin Limestone is exposed as a 50m thick section (at Grid Ref. DP202157; 42°16.4'S, 146°2.65'E) to the north side of the Everlasting Hills (Fig. 1D). Two samples (JRC 2 and JRB) from this location produced relatively abundant conodonts (Table 1). The remaining 305 specimens were recovered from five large spot samples – YYF1 (13 kg), YYF2 (8 kg), YYF3 (10 kg), YYF4 (7.5 kg), and YYF5 (11 kg) – collected from the lower part of the Lower Limestone Member of the Benjamin Limestone in the Settlement Road section of the Florentine Valley area (Figs 1C, 2).

SYSTEMATIC PALAEONTOLOGY

All photographic illustrations shown in Figures 3 to 17 are SEM photomicrographs of conodonts captured digitally (numbers with the prefix IY are the file names of the digital images). Figured specimens bearing the prefix AM F. are deposited in the type collections of the Palaeontology Section at the Australian Museum in Sydney. All the syntypes except one (UTG96863 not located; figured by Burrett 1979, pl. 1, figs 17-18) and most of the other specimens of *Tasmanognathus careyi* illustrated by Burrett (1979) were relocated and made available for the current study. They have been now transferred to the Australian Museum collection, and a new AM F. registration number has been allocated to each of the specimens illustrated in this contribution.

The following species are documented herein only by illustration as they are either rare in the collection or have been adequately described elsewhere in the literature: *Aphelognathus*? sp. (Fig. 3J-K), *Drepanodus* sp. (Fig. 3C-F), gen. et sp. indet. (Fig. 3G-I), and *Panderodus gracilis* (Branson and Mehl, 1933) (Fig. 6A-I). Authorship of the new species *Chirognathus tricostatus* is attributable solely to Zhen. Taxa documented herein are alphabetically listed according to their generic assignment, with family level and higher classification omitted.

Phylum Chordata Balfour, 1880
Class Conodonta Pander, 1856

Genus BELODINA Ethington, 1959

Type species
Belodus compressus Branson and Mehl, 1933.

Belodina compressa (Branson and Mehl, 1933)
Fig. 3A-B

Synonymy
Belodus compressus Branson and Mehl, 1933, p. 114, pl. 9, figs 15, 16.
Belodus grandis Stauffer, 1935, p. 603-604, pl. 72, figs 46, 47, 49, 53, 54, 57.
Belodus wykoffensis Stauffer, 1935, p. 604, pl. 72, figs 51, 52, 55, 58, 59.
Oistodus fornicalus Stauffer, 1935, p. 610, pl. 75, figs 3-6.
Belodina dispansa (Glenister); Schopf, 1966, p. 43, pl. 1, fig. 7.
Belodina compressa (Branson and Mehl); Bergström and Sweet, 1966, p. 321-315, pl. 31, figs 12-19; Sweet in Ziegler, 1981, p. 65-69, *Belodina* - plate 2, figs 1-4; Leslie, 1997, p. 921-926, figs 2.1-2.20, 3.1-3.4 (*cum syn.*); Zhen et al., 2004, p. 148, fig. 5A-I (*cum syn.*); Percival et al., 2006, fig. 3A-D.
Belodina confluens Sweet; Percival et al., 1999, p. 13, Fig. 8.21.

Material
Ten specimens from two samples (see Table 1).

Discussion
Only compressiform (Fig. 3A) and grandiform (Fig. 3B) elements were recovered from the Tasmanian samples. These elements are identical with those recorded from the upper part of the Wahringa Limestone Member of the Fairbridge Volcanics (assemblage C, see Zhen et al. 2004), and others from drillcore samples in the Marsden district (Percival et al. 2006) of central New South Wales. Morphological distinction between *B. compressa* and closely related species, particularly *B. confluens*, was discussed by Zhen et al. (2004).

Genus CHIROGNATHUS Branson and Mehl, 1933

Type species
Chirognathus duodactylus Branson and Mehl, 1933.

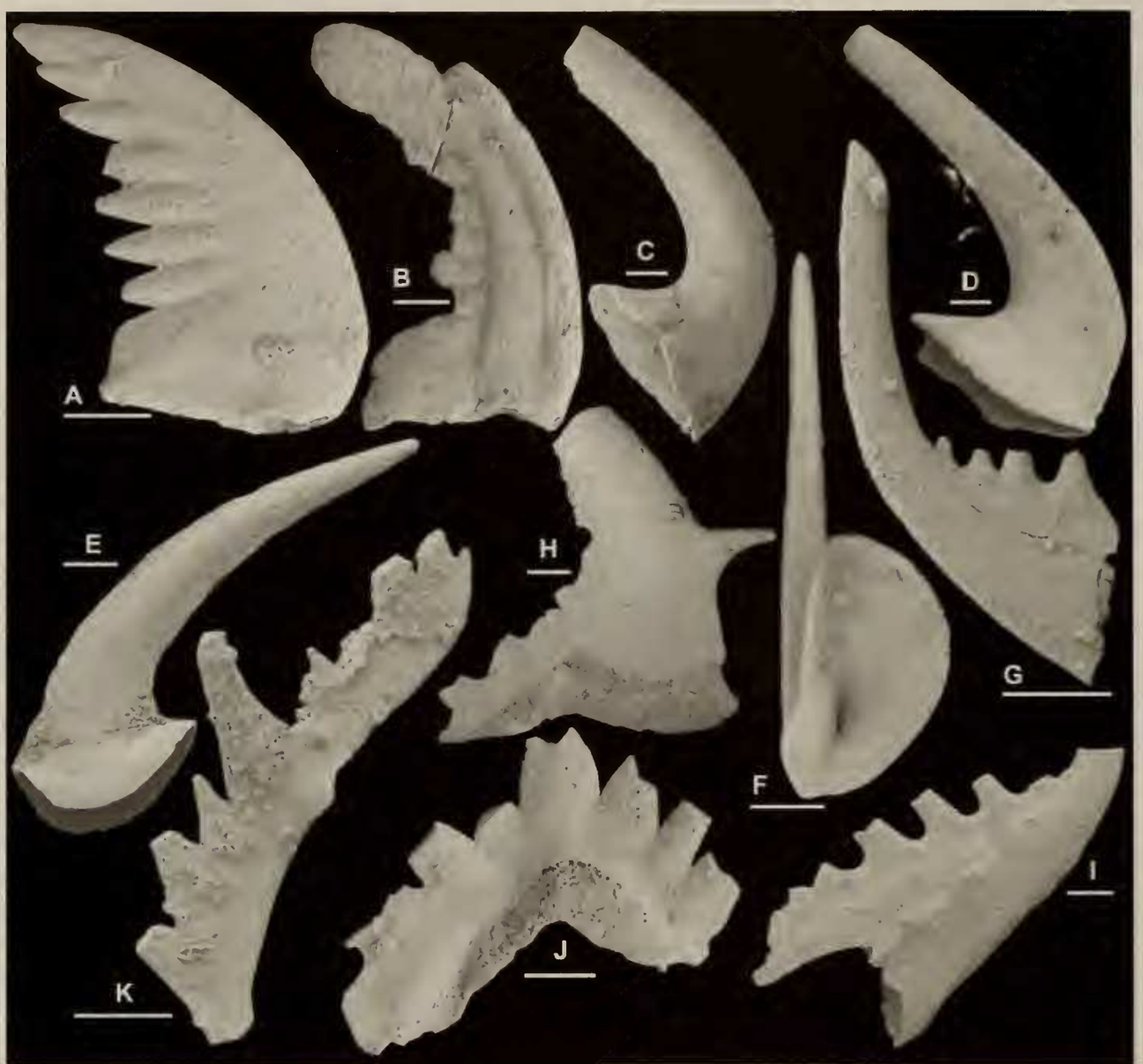

Figure 3. A-B, *Belodina compressa* (Branson and Mehl, 1933). A, compressiform element, AM F.136480, JRC 2, inner-lateral view (1Y139-001); B, grandiform element, AM F.136481, JRC 2, outer-lateral view (IY139-003). C-F, *Drepanodus* sp. C, Sb element, AM F.136482, JRC 2, outer-lateral view (1Y139-005). D, Sb element, AM F.136483, JRC 2, inner-lateral view (1Y139-006). E, F, M element, AM F.136484, JRC 2, E, inner-lateral view (1Y139-004); F, basal view (1Y139-014). G-I, Gen. et sp. indet., all from YYF4, G, Sc element, AM F.136485, inner-lateral view (1Y136-022); H, ?P element, AM F.136486, outer-lateral view (1Y136-021); I, Sb element, AM F.136487, outer-lateral view (1Y136-019). J-K, *Aphelognathus*? sp. from YYF4, J, Pb element, AM F.136488, inner-lateral view (1Y135-025). K, Pa element, AM F.136489, inner-lateral view (1Y136-024). Scale bars 100 µm.

Discussion

Chirognathus was established on 23 form species recognized by Branson and Mehl (1933, pp. 28-34, pl. 2) from the Harding Sandstone in Canyon City, Colorado with *Chirognathus duodactylus* as the type species. Later Stauffer (1935) erected 15 form species of *Chirognathus* from the upper Glenwood Beds in the upper Mississippi Valley. Sweet (1982) revised the type species as having a seximembrate or septimembrate apparatus, and concluded that the 29 out of the 42 species recognized by Branson and Mehl (1933), Stauffer (1935), and others since the establishment of the genus could be confidently assigned to the genus, and in fact might belong to a single species apparatus of his revised *C. duodactylus*. He regarded 15 of Branson and Mehl's (1933) and 13

of Stauffer's (1935) form species as junior synonyms of *C. duodactylus*, with the M element represented by form species *C. duodactylus* (= *C. gradatus* Branson and Mehl, 1933, = *C. planus* Branson and Mehl, 1933), Sa by form species *C. multidens* Branson and Mehl, 1933, Sb by form species *C. panneus* Branson and Mehl, 1933 (= *C. isodactylus* Branson and Mehl, 1933), Sc by form species *C. eucharis* Stauffer, 1935, Pa by form species *C. varians* Branson and Mehl, 1933 (= *C. alternatus* Branson and Mehl, 1933), and Pb by form species *C. monodactylus* Branson and Mehl, 1933 (= *C. reversus* Branson and Mehl, 1933). As defined by Sweet (1982, p. 1039), *C. duodactylus* has a ramiform-ramiform species apparatus including a bipennate M element with a short and laterally deflected anterior process and a long posterior process, an alate Sa element with a straight, laterally extended lateral process on each side, a digyrate Sb element varying from subsymmetrical (with two processes subequal in length) to markedly asymmetrical (with one lateral process longer than the other), a bipennate Sc element with a shorter anterior process, a bipennate Pa element resembling the Sc but with the unit inwardly bowed with a more prominently arched basal margin, and a digyrate Pb element with two lateral processes directed in opposite directions distally.

Chirognathus cliefdenensis Zhen and Webby, 1995, from the Cliefden Caves Limestone Subgroup of central New South Wales, differs from *C. duodactylus* in having distinctive blade-like P elements with high processes bearing closely spaced, basally confluent denticles (Zhen and Webby 1995, pl. 2, figs 13-16).

Chirognathus tricostatus sp. nov.
Figs 4-5

Synonymy

Chirognathus monodactyla Branson and Mehl; Burrett, 1979, pp. 31-32.

Tasmanognathus careyi Burrett, 1979, p. 33-35, *partim*, only pl. 1, fig. 12.

Derivation of name

Latin *tri-* (three) and *costatus* (ribbed) referring to the distinctive character, the tricostate cusp of the Sb, Sc and Sd elements, of this Tasmanian species.

Material

71 specimens from eight samples (see Table 1). Holotype: AMF.136496, YYF5, Sd element (Fig. 5A-C); paratypes: AM F.136490, C137c, Sa element (Fig. 4A-C); AM F.136491, JRC 2, Sa element (Fig. 4D); AM F.136492, YYF5, Sb element (Fig. 4E); AM F.136493, C137c, Sb element (Fig. 4F); AM F.136494 (=UTG96872: Burrett 1979, pl. 1, fig. 12; originally designated as one of the syntypes of *T. careyi*), Sb element (Fig. 4G-H); AM F.136495, YYF5, Sc element (Fig. 4I-J); AM F.136497, C137c, Sd element (Fig. 5D-E); AM F.136498, C137c, Sd element (Fig. 5F-G); AM F.136499, JRC 2, Pa? element (Fig. 5H); AM F.136500 (=UTG96866), JRC 2, Pa element (Fig. 5I); AM F.136501, JRC 2, Pa element (Fig. 5J-K); AM F.136502, YYF1, Pb element (Fig. 5L-N); AM F.136503, YYF4, Pb element (Fig. 5O).

Diagnosis

A species of *Chirognathus* with a seximembrate (possibly septimembrate) ramiform-ramiform apparatus including alate Sa, modified digyrate Sb and Sd, modified bipennate Sc, bipennate Pa and digyrate Pb elements; all elements with long, peg-like denticles, and a shallow, open basal cavity, typically preserved without attachment of a basal funnel.

Description

Sa element symmetrical or nearly symmetrical, with a prominent cusp and a denticulate lateral process on each side (Fig. 4A-D); cusp large, straight, antero-posteriorly compressed, with broadly convex anterior and posterior faces and sharply costate lateral margins; lateral processes extending laterally and bearing three or more denticles of variable sizes, which are also antero-posteriorly compressed; basal cavity flared anteriorly and posteriorly with basal margin nearly straight or slightly arched in posterior or anterior view (Fig. 4A, D).

Sb element (Fig. 4E-H) like Sa, but asymmetrical with outer lateral process slightly curved posteriorly and with a short, but prominent costa developed on the basal part of the anterior face (Fig. 4E, H); outer lateral process slightly curved posteriorly and also with basal margin twisted posteriorly and upper margin anteriorly (Fig. 4G); basal cavity shallow, flared anteriorly and posteriorly and extending distally as a narrow and shallow groove underneath each process (Fig. 4F).

Sc element modified bipennate, strongly asymmetrical with denticulate anterior and posterior processes and a strong costa on the outer lateral face (Fig. 4I-J); both processes extending straight or slightly curved inward; anterior process bearing three or more denticles with the distal denticle (away from the cusp) larger than the other denticles; posterior process bearing two or more denticles with the distal one (away from the cusp) larger than the other denticle; larger denticle on the posterior or anterior

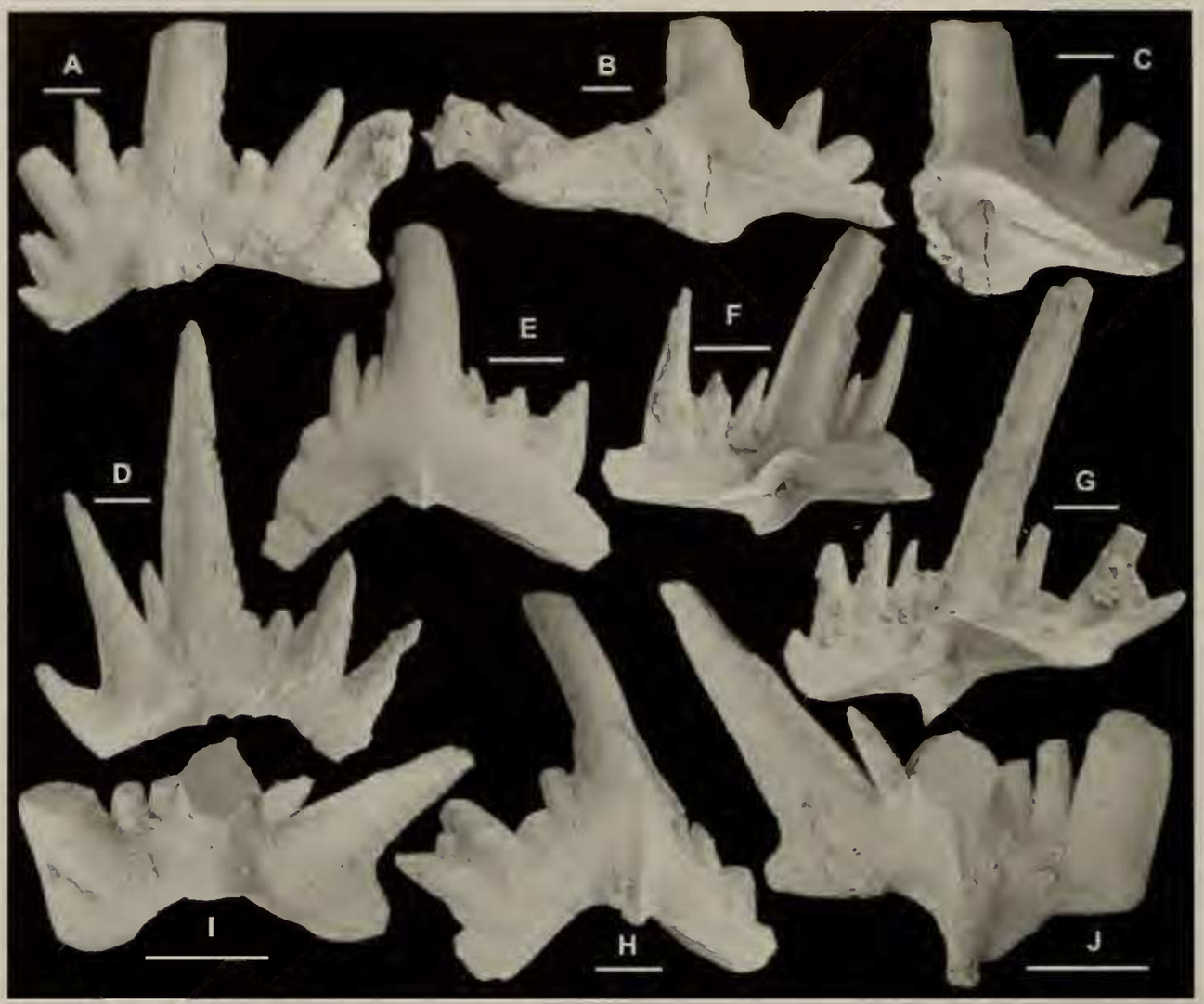

Figure 4. ***Chirognathus tricostatus*** **sp. nov. A-D, Sa element; A-C, AM F.136490, paratype, C137c, A, anterior view (IY138-020), B, basal view (IY138-021), C, posterior view (IY142-023); D, AM F.136491, paratype, JRC 2, anterior view (IY142-002). E-H, Sb element; E, AM F.136492, paratype, YYF5, anterior view (IY135-039); F, AM F.136493, paratype, C137c, posterior view (IY138-022); G-H, AM F.136494=UTG96872 (Burrett 1979, pl. 1, fig. 12; originally designated as one of the syntypes of T. careyi), paratype, JRC 2, G, posterior view (IY141-018), H, anterior view (IY141-019). I-J, Sc element, AM F.136495, paratype, YYF5, I, upper-inner lateral view (IY135-035), J, upper-outer lateral view (IY135-036). Scale bars 100 µm.**

process being as wide as the cusp in the lateral view, but more strongly compressed laterally than the cusp; outer lateral costa prominent, forming a ridge-like process near the base (Fig. 4J).

Sd element modified digyrate, strongly asymmetrical with a robust cusp, a denticulate lateral process on each side and a blade-like costa on the anterior face (Fig. 5A-G); cusp tricostate with a sharp costa along the lateral margins and on the broadly convex anterior face, and a less convex posterior face; anterior costa more strongly developed than that in the Sb element, and extending to near the tip of the cusp, and basally often developed into a short, blade-like process (Fig. 5C-D, G); lateral processes distally curved posteriorly bearing three or more denticles of variable sizes; basal cavity more open and strongly flared posteriorly than that of the Sb element, forming a strongly arched basal margin in posterior view (Fig. 5F).

Pa element bipennate with a prominent cusp and denticulate anterior and posterior processes (Fig. 5H-K); cusp suberect, laterally compressed with sharply costate anterior and posterior margins and broadly convex lateral faces (Fig. 5H-J); both anterior and posterior processes bearing three or more denticles of variable sizes, which are also laterally compressed;

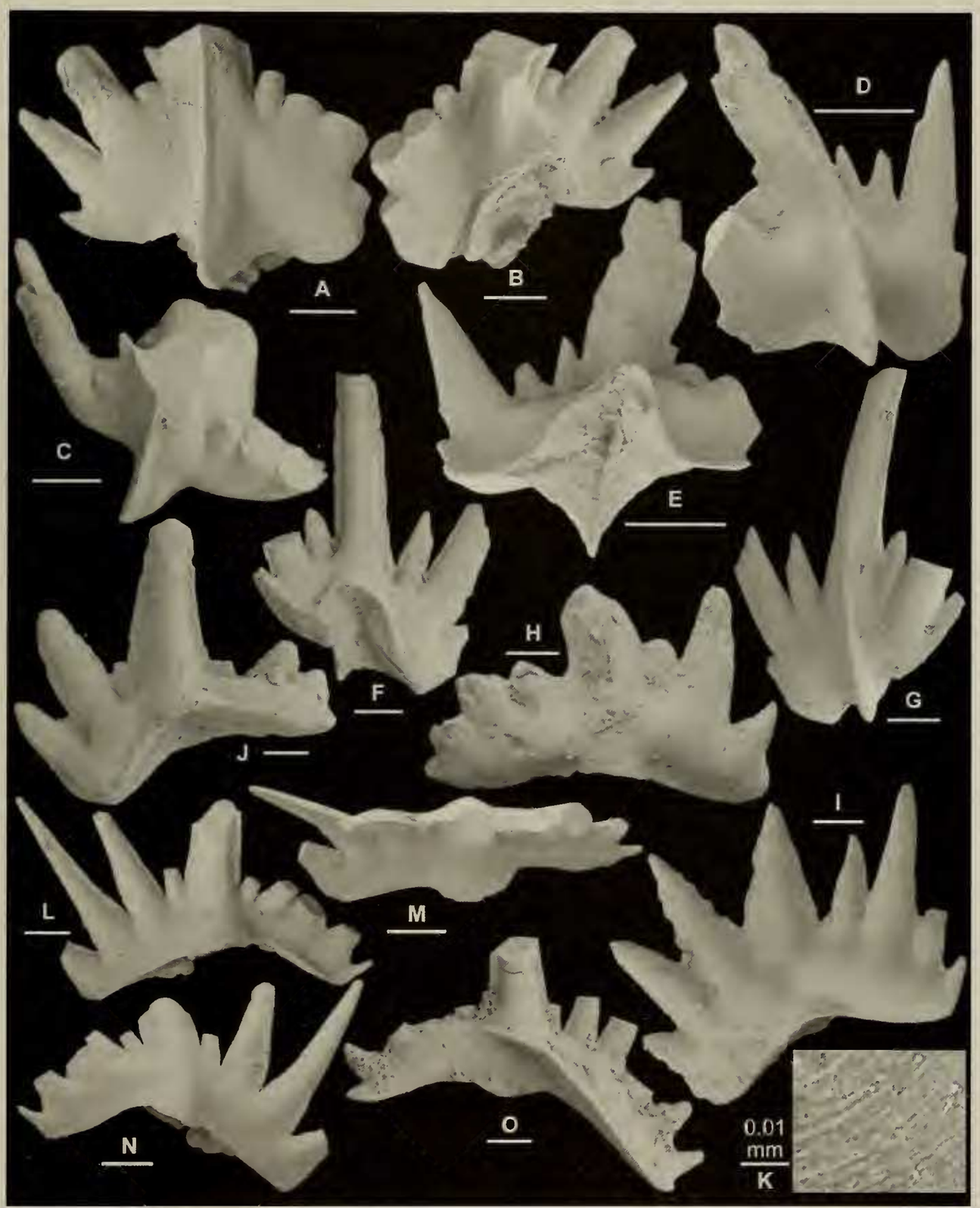

Figure 5. ***Chirognathus tricostatus*** **sp. nov. A-G, Sd element; A-C, AM F.136496, Holotype, YYF5, A, anterior view (IY135-034), B, posterior view (IY142-028), C, upper view (IY135-033); D-E, AM F.136497, paratype, C137c, D, anterior view (IY142-025), E, posterior view (IY138-027); F-G, AM F.136498, paratype, C137c, F, posterior view (IY138-024), G, anterior view (IY142-026). H, Pa? element; AM F.136499, paratype, JRC 2, outer lateral view (IY142-018); I-K, Pa element, I, AM F.136500 =UTG96866, paratype, JRC 2, outer lateral view (IY141-026); J-K, AM F.136501, paratype, JRC 2, J, inner lateral view (IY142-020), K, basal view, close up showing the zone of recessive basal margin (IY142-022). L-O, Pb element; L-N, AM F.136502, paratype, YYF1, L, posterior view (IY136-30), M, upper view (IY136029), N, anterior view (IY142-029); O, AM F.136503, paratype, YYF4, basal-posterior view (IY135-026). Scale bars 100 μm.**

Fig. 6. A-I, *Panderodus gracilis* (Branson and Mehl, 1933). A, falciform, AM F.136504, JRC 2, outer-lateral view (IY139-033). B-C, truncatiform element, AM F.136505, JRC 2, B, posterior view (IY139-026); C, inner-lateral view (IY139-024). D-G, graciliform element; D-F, AM F.136506, JRC 2, D, inner-lateral view (IY139-017); E, outer-basal view of the basal part (IY139-022); F, outer-lateral view (IY139-020); G, AM F.136507, JRC 2, outer-lateral view (IY139-023). H-I, falciform element; H, AM F.136508, JRC 2, inner-lateral view (IY139-035); I, AM F.136509, YYF2, outer-lateral view (IY140-25). J-N, Protopanderodus? nogamii (Lee, 1975). J, Sb element, AM F.136510, YYF4, outer-lateral view (IY136-027). K-N, Pa element; K-L, AM F.136511, YYF4, K, outer-lateral view (IY136-025), L, outer lateral view, closer up showing the furrow weaken and disappeared before researching basal margin (IY136-026). M-N, AM F.136512, YYF3, M, outer-lateral view (IY140-021), N, basal view (IY140-019). Scale bars 100 μm unless otherwise indicated.

anterior process typically slightly curved inward and extending downward forming a gently arched basal margin in lateral view (Fig. 5I-J); basal cavity shallow and open, often with zone of recessive basal margin preserved (Fig. 5K).

Pb element digyrate with a prominent cusp and denticulate lateral process on each side (Fig. 5L-O); cusp curved posteriorly with costate lateral margins; lateral processes bearing four or more denticles of variable sizes; basal cavity shallow and open with gently arched basal margins in anterior or posterior view (Fig. 5L, N-O).

Discussion

Chirognathus tricostatus sp. nov. was initially reported by Burrett (1979) as *Chirognathus monodactyla*, one of the 23 form species recognized by Branson and Mehl (1933). One of the syntypes of *Tasmanognathus careyi* (AM F.136494 =UTG 96872) is re-assigned herein to *C. tricostatus* to represent

the Sb position (Fig. 4G; also see Burrett 1979, pl. 1, fig. 12). *C. tricostatus* from Tasmania differs from two currently known multi-element species of *Chirognathus*, *C. duodactylus* from the Upper Ordovician (Sandbian) of North American Mid-continent faunas and *C. cliefdenensis* from the Upper Ordovician (Katian) of central New South Wales, in having distinctive tricostate Sb, Sc and Sd elements.

Sweet (1982, 1988) recognized the M element for the type species, *C. duodactylus*. A comparable element has also recognized in the Tasmanian material of *C. tricostatus*, but has been assigned to the Sd position to form a symmetry transitional series with other S elements. One of the illustrated specimens of the Pa element (Fig. 5H) shows a nearly straight basal margin and posteriorly curved cusp, and may possibly represent the M element of this species. However, as only one specimen is available in the current material, it is tentatively assigned to the Pa element.

Genus PHRAGMODUS Branson and Mehl, 1933

Type species

Phragmodus primus Branson and Mehl, 1933.

Phragmodus undatus Branson and Mehl, 1933

Figs 7-8

Synonymy

Phragmodus undatus Branson and Mehl, 1933, p. 115-116, pl. 8, figs 22-26; Zhen and Webby, 1995, p. 284, pl. 4, fig. 5; Leslie and Bergström, 1995, p. 970-973, fig. 4.1-4.14 (*cum syn.*); Zhen et al., 1999, p. 90, fig. 9.1-9.5 (*cum syn.*); Zhen et al., 2003a, fig. 6N, O; Pyle and Barnes, 2002, figs 14.11-14.12, 15.31-15.32; Percival et al., 2006, fig. 4A-E.

Material

116 specimens from six samples (see Table 1).

Description

M element makellate, geniculate coniform with a robust cusp and a short base triangular in outline (Fig. 7A-B); cusp strongly antero-posteriorly compressed forming sharp lateral edges and broad anterior and posterior faces; inner-lateral corner triangular in outline, and outer-lateral proto-process short with a gently arched upper margin; basal cavity shallow with weakly wavy basal margins.

S elements ramiform bearing a long multi-denticulate posterior process with one or two enlarged denticles, but none of the Tasmanian specimens have the posterior process completely preserved. Sa element symmetrical or nearly symmetrical with a prominent costa on each side (Fig. 7C-D); posterior process long with one denticle (typically the third or fourth from the cusp) about twice as wide as the adjacent denticles, and larger and longer than the cusp; in some specimens a costa also developed on each side of the larger denticle (Fig. 7D); basal cavity shallow with strongly arched basal margins; anterior (or antero-inner lateral) costa typically only weakly developed (Fig. 7D). Sb element modified quadriramate, like Sa but asymmetrical with the sharp costate anterior margin curved inward (Fig. 7F-G). Sc element modified bipennate, like Sb but strongly asymmetrical with a sharply costate anterior margin curved inward and with smooth inner and outer lateral faces (Fig. 7H-L). Sd element tertiopedate, like Sb, but with a broad anterior face and with one of the larger denticles on the posterior process curved inward and the other outward (Fig. 8A-C).

Pa element pastinate with long denticulate posterior and inner lateral processes, and a suberect cusp (Fig. 8D-G); cusp laterally compressed with sharply costate anterior and posterior margins, outer lateral face more convex; posterior process long, bearing six or more denticles; inner lateral process shorter, bearing five or more denticles and strongly bending anteriorly forming an angle of nearly 180 degree with the posterior process (Fig. 8E, G); costate anterior margin extending downward and not forming a prominent anterior process (Fig. 8D); basal cavity shallow, forming a wide and open groove along the posterior and inner lateral processes, and flared anteriorly and inner laterally (Fig. 8G). Pb element pastinate, like Pa but with a more robust cusp and less anteriorly curved inner lateral process (Fig. 8H-I).

Discussion

Leslie and Bergström (1995) suggested a seximembrate apparatus for *P. undatus*, including adenticulate makellate M, alate Sa, tertiopedate Sb, bipennate Sc, pastinate Pa and Pb elements. All six elements have been recovered from the Tasmanian samples (Figs 7-8); they are identical with those described and illustrated by Leslie and Bergström (1995, fig. 4) from the Joachim Dolomite and Kings Lake Limestone of Missouri, except that an additional tertiopedate element was recognized in the Tasmanian material (Fig. 8A-C). This latter element is similar to the Sb element, but has the cusp and the larger denticles on the posterior process strongly twisted towards different sides in respect to the antero-posterior axis. It is assigned herein to represent the Sd position.

Fig. 7. ***Phragmodus undatus*** **Branson and Mehl, 1933. A-B, M element; A, AM F.136513, YYF4, posterior view (IY136-005); B, AM F.136514, YYF4, anterior view (IY136-006). C-D, Sa element, AM F.136515, C137c, C, basal view (IY138-014); D, lateral view (IY138-015). E-G, Sb element; E, AM F.136516, YYF4, outer-lateral view (IY136-015); F, AM F.136517, YYF4, inner-lateral view (IY136-014), G, AM F.136518, YYF4, inner-lateral view (IY136-016). H-L, Sc element; H, AM F.136519, YYF4, inner-lateral view (IY136-013); I-J, AM F.136520, YYF4, I, outer-lateral view (IY136-009), J, inner-lateral view (IY136-010); K-L, AM F.136521, C137c, K, basal view (IY138-016), L, outer-lateral view (IY138-017). Scale bars 100 µm.**

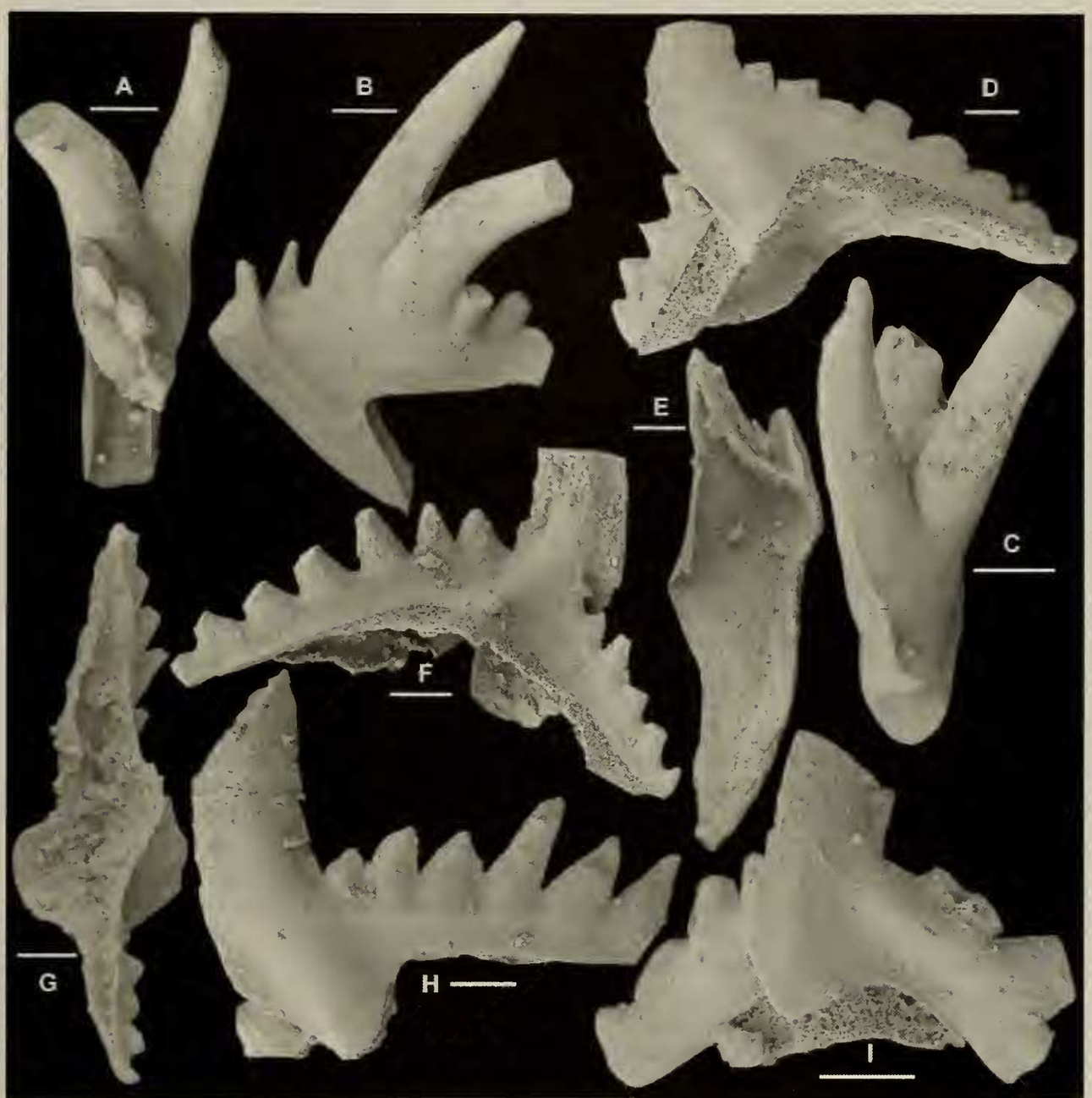

Fig. 8. ***Phragmodus undatus*** **Branson and Mehl, 1933. A-C, Sd element; AM F.136522, JRC 2, A, upper view (IY138-028), B, outer-lateral view (IY138-029), C, posterior view (IY138-030). D-G, Pa element; D-E, AM F.136523, YYF4, D, outer-lateral view (IY136-001), E, basal view (IY136-011); F-G, AM F.136524, YYF4, F, inner-lateral view (IY136-003), G, basal view (IY136-012). H-I, Pb element; H, AM F.136525, YYF4, outer-lateral view (IY136-004); I, AM F.136526, YYF4, antero-outer lateral view (IY136-017). Scale bars 100 µm.**

Genus PROTOPANDERODUS Lindström, 1971

Type species

Acontiodus rectus Lindström, 1955.

Protopanderodus? *nogamii* (Lee, 1975)
Fig. 6J-N

Synonymy

Scolopodus nogamii Lee 1975, p. 179, pl. 2, fig. 13.

?*Panderodus nogamii* (Lee); Cantrill and Burrett 2004, p. 410, pl. 1, figs 1-16.

Panderodus nogamii (Lee); Zhang et al. 2004, p. 16, pl. 5, figs 1-5.

Protopanderodus nogamii (Lee); Watson 1988: p. 124, pl. 3, figs 1, 6; Zhen et al. 2003b, p. 207-

209, fig. 23A-P, ?Q (*cum syn.*); Zhen and Percival 2004a, p. 104-105, fig. 18A-K (*cum syn.*).
Protopanderodus? nogamii (Lee); Zhen and Percival 2004b, p. 170-172, fig. 11P, Q (*cum syn.*).

Material

69 specimens from four samples (see Table 1).

Discussion

Recent review of this species by Cantrill and Burrett (2004) suggested a geographical distribution restricted to Gondwana and peri-Gondwanan terranes. Morphologically *P. nogamii* is rather conservative over its long stratigraphic range from the upper Floian (*evae* Zone, Zhen et al. 2003b) to upper Sandbian (*undatus* Zone, this study). Generic assignment of this species has been debated in the literature (see synonymy list). Most elements of this species bear a non-panderodontid furrow on each side, suggesting that it might be more closely related to *Protopanderodus* rather than to typical *Panderodus*.

Genus TASMANOGNATHUS Burrett, 1979

Type species

Tasmanognathus careyi Burrett, 1979.

Diagnosis

Septimembrate apparatus with a ramiform-pectiniform apparatus structure including makellate M, ramiform S (including alate Sa with a denticulate lateral process on each side, digyrate Sb, bipennate or modified bipennate Sc, and tertiopedate Sd), carminate Pa, and angulate Pb (some species with an additional modified angulate or pastinate Pb2) elements.

Discussion

Following Burrett's (1979, p. 32) original view that *Tasmanognathus* might be closely related to *Rhipidognathus*, Aldridge and Smith (1993) doubtfully included it in the Rhipidognathidae. Affinities with other genera remain conjectural, although greatest similarities appear to be with *Yaoxianognathus* (see discussion below).

Tasmanognathus was established on a single species, *T. careyi* Burrett, 1979 from the Lower Member of the Benjamin Limestone in the Florentine Valley and Everlasting Hills of central Tasmania. Subsequently, *Tasmanognathus* has been reported from the mid Darriwilian to upper Katian of eastern Australia, North China (An et al. 1985, An and Zheng 1990, Pei and Cai 1987), Qinling Mountains in the Kunlun-Qinling Region (Pei and Cai 1987), Tarim Basin (Zhao et al. 2000; Jing et al. 2007), South Korea (Lee 1982; An and Zheng 1990), ?Siberia and northeastern Russia (Domoulin et al. 2002), and possibly North America (where it was referred to as *Yaoxianognathus abruptus*). It is represented by nine named species and several additional unnamed forms, the latter included herein in *Tasmanognathus* although some are poorly known or inadequately documented. Following is a brief review of the known species (with our interpretation of element notations in parentheses):

Tasmanognathus careyi Burrett, 1979 from the Lower Limestone Member of the Benjamin Limestone in the Florentine Valley and Everlasting Hills of central Tasmania; a seximembrate apparatus was originally recognized, but based on re-examination of original topotypes and additional new material, it has been revised herein as having an septimembrate apparatus (including M, Sa, Sb, Sc, Sd, Pa, and Pb elements).

Badoudus badouensis Zhang in An et al., 1983 from the Fengfeng Formation (Sandbian) of Handan, Hebei Province in North China (considered by An et al. 1985, p. 102, to represent a species of *Tasmanognathus*); this is a poorly defined form species with only two specimens illustrated (An et al. 1983, pl. 25, figs 5, 6, text-fig. 12.17), both of which are carminate, bearing an indistinctive cusp and a long denticulate anterior process and a short denticulate posterior process. This element is comparable with the Pa element of *Tasmanognathus* defined herein.

Tasmanognathus borealis An in An et al., 1985 from the upper part of the Yaoxian Formation (late Sandbian) of Yaozhou District (formerly Yaoxian) of Tongchuan City, Shaanxi Province in North China; originally defined as having a quinquimembrate apparatus, including trichonodelliform (= Sa element; see An et al. 1985, pl. 1, fig. 20), zygognathiform (= Sb element; see An et al. 1985, pl. 1, fig. 13), cordylodiform (= Sc element; see An et al. 1985, pl. 1, fig. 15), ozarkodiniform (= Pa element; see An et al. 1985, pl. 1, fig. 14), and prioniodiniform (= Pb element; see An et al. 1985, pl. 1, fig. 16).

Tasmanognathus gracilis An in An et al., 1985 from the upper part of the Yaoxian Formation (late Sandbian) of Yaozhou District (formerly Yaoxian) of Tongchuan City, Shaanxi Province in North China; originally defined as having a seximembrate apparatus, including cyrtoniodiform (= M element; see An et al. 1985, pl. 1, fig. 8), trichonodelliform (= Sa element; see An et al. 1985, pl. 1, fig. 12), ligonodiniform (= Sb element; see An et al. 1985, pl. 1, fig. 11), cordylodiform (= Sc element; see An et al. 1985, pl. 1, fig. 10), ozarkodiniform (= Pa element;

see An et al. 1985, pl. 1, fig. 7), and prioniodiniform (= Pb element; see An et al. 1985, pl. 1, fig. 9).

Tasmanognathus multidentatus An in An and Zheng, 1990 (p. 20, 95, text-fig. 9, pl. 11, fig. 4); the only figured specimen (pl. 11, fig. 4) is a Pa element from the Yaoxian Formation of Yaozhou District (formerly Yaoxian) of Tongchuan City, Shaanxi Province in North China, which is identical with the Pa element of *T. borealis* An in An et al., 1985. In fact, the figured Pa element (pl. 11, fig. 4) of *T. multidentatus* and the holotype and a figured paratype of *T. borealis* (An et al. 1985, pl. 1, figs 13, 16) were recovered from the same sample (Tp13y2). It is unclear why An and Zheng (1990) tried to replace *T. borealis* with *T. multidentatus*. However, as the latter is a *nomem nudum*, *T. borealis* remains the valid name for this Yaoxian species.

Tasmanognathus planatus Pei in Pei and Cai, 1987 from the Sigang Formation of Xichuan and Neixiang Counties, Henan Province in the Qinling Mountains (Pei and Cai 1987; Chen et al. 1995; Wang et al. 1996); the type material was represented by Pa (Pei and Cai 1987, pl. 13, fig. 12), Pb (Pei and Cai 1987, pl. 13, figs 8, ?13), and Sb (Pei and Cai 1987, pl. 13, fig. 9) elements.

Tasmanognathus shichuanheensis An in An et al., 1985 from the lower part of the Yaoxian Formation (mid Sandbian) of Yaozhou District (formerly Yaoxian) of Tongchuan City, Shaanxi Province in North China; originally defined as having a seximembrate apparatus, including cyrtoniodiform (= M element; see An et al. 1985, pl. 1, fig. 3), trichonodelliform (= Sa element; see An et al. 1985, pl. 1, fig. 4), ligonodiniform (= Sb element; see An et al. 1985, pl. 1, fig. 1), cordylodiform (= Sc element; see An et al. 1985, pl. 1, fig. 5), ozarkodiniform (= Pa element; see An et al. 1985, pl. 1, fig. 2), and prioniodiniform (= Pb element; see An et al. 1985, pl. 1, fig. 6).

Tasmanognathus sigangensis Pei in Pei and Cai, 1987 from the Shiyanhe Formation (late Sandbian-early Katian) of Neixiang County, Henan Province in the Qinling Mountains; a quinquimembrate species apparatus was recognized including trichnodelliform (= Sa element; Pei and Cai 1987, pl. 13, fig. 4), zygognathiform (= Sb element, Pei and Cai 1987, pl. 13, fig. 11), cordylodontiform (= Sc element; Pei and Cai 1987, pl. 13, fig. 7), prioniodiniform (= Pa element; Pei and Cai 1987, pl. 13, figs 1-2), and ozarkodontiform (= ?Pb element; Pei and Cai 1987, pl. 13, fig. 3).

Tasmanognathus sishuiensis Zhang in An et al., 1983 reported from the upper Fengfeng Formation (early Sandbian) of Shandong and Hebei provinces in North China; defined as consisting of a quinquimembrate apparatus including trichonodelliform (= Sa element, see An et al. 1983, pl. 29, figs 7, 9, 10), zygognathiform (= Sb element, see An et al. 1983, pl. 29, figs 4-6, 8, ?11), cordylodontiform (= Sc element, see An et al. 1983, pl. 29, figs 1-3), ozarkodiniform (= Pa element, see An et al. 1983, pl. 29, figs 14-15), and prioniodiniform (= Pb element, see An et al. 1983, pl. 29, figs 12-13) elements. This species is characterized by its widely spaced peg-like denticles on the S elements.

Tasmanognathus sp. described by Pei and Cai (1987) from the Sigang and Shiyanhe formations of Neixiang County, Henan Province in the Qinling Mountains; represented by cordylodontiform (= Sc element; Pei and Cai 1987, pl. 13, figs 5-6) and prioniodiniform (= ?Pb element; Pei and Cai 1987, pl. 13, fig. 10) elements.

Tasmanognathus sp. from the Fossil Hill Limestone (early Katian) of the Cliefden Caves Limestone Subgroup, central New South Wales was only represented by the Pa element (Zhen and Webby 1995, p. 289, pl. 5, fig. 23), which showed close resemblance to the Pa element of *T. borealis* from the Yaoxian Formation.

Tasmanognathus sp. cf. *T. borealis* An in An et al., 1985; only the Pa element known from unnamed limestone of Late Ordovician (late Sandbian) age intersected in drillcore in the Marsden district of south-central New South Wales (Percival et al. 2006).

The three species of *Tasmanognathus* (*T. borealis, T. gracilis* and *T. shichuanheensis*) erected by An in An et al. (1985) from the Yaoxian Formation (Darriwilian-Sandbian) of Yaozhou District (formerly Yaoxian) of Tongchuan City, Shaanxi Province in North China exhibit similar species apparatus and closely related morphological variations of constituent elements. An et al. (1985) established two conodont zones in the Yaoxian Formation, namely the *T. shichuanheensis* Zone in the lower part of the formation (Bed 1 to Bed 3, see An et al. 1985, fig. 2), and the *Tasmanognathus borealis-T. gracilis* Zone spanning the upper part of the Yaoxian Formation (Bed 4 to Bed 8) into the basal part of the overlying Taoqupo Formation (Bed 9). An and Zheng (1990, p. 95, text-fig. 9) suggested that *T. sishuiensis* from the Fengfeng Formation might be the direct ancestor of the species from the Yaoxian Formation, and indicated an inferred lineage from *T. sishuiensis* to *T. shichuanheensis* and then to *T. multidentatus* (= *T. borealis*). They showed the morphological changes of the three species, mainly from widely spaced denticles on the processes of the S and Pb elements and a prominent cusp on the Pa

element of *T. sishuiensis*, to closely spaced denticles in the S and Pb elements and an indistinctive cusp in the Pa element of *T. multidentatus* (= *T. borealis*). However, these species from the Yaoxian Formation and Fengfeng Formation show some detailed differences in composition of the apparatus in comparison with *T. careyi* from Tasmania. In particular, they seem to lack makellate M and tertiopedate Sd elements, and have a "dolabrate" Sc element with a long denticulate posterior process. Morphologically, such features support a closer relationship with *Yaoxianognathus yaoxianensis* An in An et al., 1985. However, these species lack hindeodellid denticles on the processes of the S elements, which was the major character that An (in An et al. 1985) employed to distinguish *Yaoxianognathus* from *Tasmanognathus*. As revision of An's species of *Tasmanognathus* from the Yaoxian Formation and the Fengfeng Formation of North China is beyond the scope of the current study, they are retained in *Tasmanognathus* for the time being, although they show some significant differences in morphology and apparatus composition in comparison with the type species of *Tasmanognathus* as revised here.

Based on the concept of *Yaoxianognathus* employed by An (in An et al. 1985) and others (e.g. Savage 1990; Zhen et al. 1999), generic assignment of species previously included in *Yaoxianognathus* but which apparently lack hindeodellid denticles on the processes of the S elements, should be reconsidered. For example, *Yaoxianognathus abruptus* (Branson and Mehl, 1933), a North American Midcontinent species ranging across the *undatus* to *tenuis* zones of the Mohawkian, was initially proposed as a form species based only on a carminate Pa element (Branson and Mehl, 1933, pl. 6, fig. 11) and revised by Leslie (2000, p. 1143) as having a seximembrate apparatus. It closely resembles An's species of *Tasmanognathus* from North China; most importantly, none of Leslie's illustrated S elements of *Y. abruptus* (fig. 4.15-4.18) bears hindeodellid denticles that are characteristic of *Yaoxianognathus*, and hence we suggest this species more likely belongs to *Tasmanognathus*.

Similarly, S elements of *Yaoxianognathus? neonychodonta* Zhang, Barnes and Cooper, 2004, from the Stokes Siltstone of the Amadeus Basin in central Australia, lack hindeodellid denticles and therefore should be excluded from *Yaoxianognathus*. As Zhang et al. (2004) implied, this species may be more closely related to *Plectodina*, judging from the morphological characters of its ramiform S and pastinate Pb elements.

In comparison, the two multielement species of *Yaoxianognathus* from the Upper Ordovician of central New South Wales (*Y. wrighti* Savage, 1990 and *Y. ani* Zhen, Webby and Barnes, 1999) do exhibit well developed hindeodellid denticles on the processes of the S elements, particularly on the long posterior process of the Sc element (Savage 1990, fig. 6.7-6.12; Zhen et al. 1999, fig. 15.3-15.6, 15.9-15.12, 15.16). The apparatuses of both species include a makellate M and a modified bipennate Sc elements, which differ morphologically from corresponding elements in the *T. careyi* apparatus as defined herein.

Tasmanognathus careyi Burrett, 1979
Figures 9-15

Synonymy

Tasmanognathus careyi Burrett, 1979, p. 33-35, *partim* only text-figs 2-4, pl. 1, figs 1-7, 11, 13-19 (text-fig. 2 = Pb2 , text-fig. 3 = Pa, text-fig.4A = Sb, text-fig. 4B = Sc, text-fig. 4C, D = Sd; pl. 1, figs 1-3 = Pb2, 4-5 = Pb1, 6-7 = Pa, fig. 11 = Sc, figs 13-14= Sb, figs 15-18 = Sd, fig. 19 = Sa); *non* fig. 12 = *C. tricostatus* sp. nov., *non* figs 8-10, 20 = *T.* sp. cf. *careyi*.

? *Tasmanognathus careyi* Burrett; An and Zheng, 1990, pl. 11, fig. 2.

Material

297 specimens from nine samples (see Table 1).

Burrett (1979, p. 33, pl. 1, figs 1-7, 11-12, 17-18, 20) designated 11 figured specimens from sample JRC 2 as syntypes, ten of which (excluding UTG 96863 which was not able to be located for this study; figured by Burrett 1979, pl. 1, figs 17-18), and 225 additional specimens (including originally undesignated topotypes) from five samples (LLMB, C137, C98, JRC 2 and JRB, see Table 1) are available for the current study. AM F.136547 (=UTG 96851; Burrett 1979, pl. 1, fig. 6) representing a Pa element is selected herein as lectotype (Fig. 14A-B); and seven out of ten originally designated and illustrated syntypes were examined and illustrated herein as paralectotypes, including AM F.136557 (=UTG 96857, Fig. 15H; Burrett 1979, pl. 1, fig. 1), AM F.136559 (=UTG 96860, Fig. 15K; Burrett 1979, pl. 1, fig. 2), AM F.136560 (=UTG 96853, Fig. 15L; Burrett 1979, pl. 1, fig. 3), AM F.136553 (=UTG 96850, Fig. 15A-B; Burrett 1979, pl. 1, fig. 4), AM F.136554 (=UTG 96882, Fig. 15C; Burrett 1979, pl. 1, fig. 5), AM F.136548 (=UTG 96856, Fig. 14C; Burrett 1979, pl. 1, fig. 7), and AM F.136539 (=UTG 96876, Fig. 12A-C; Burrett 1979, pl. 1, fig. 11).

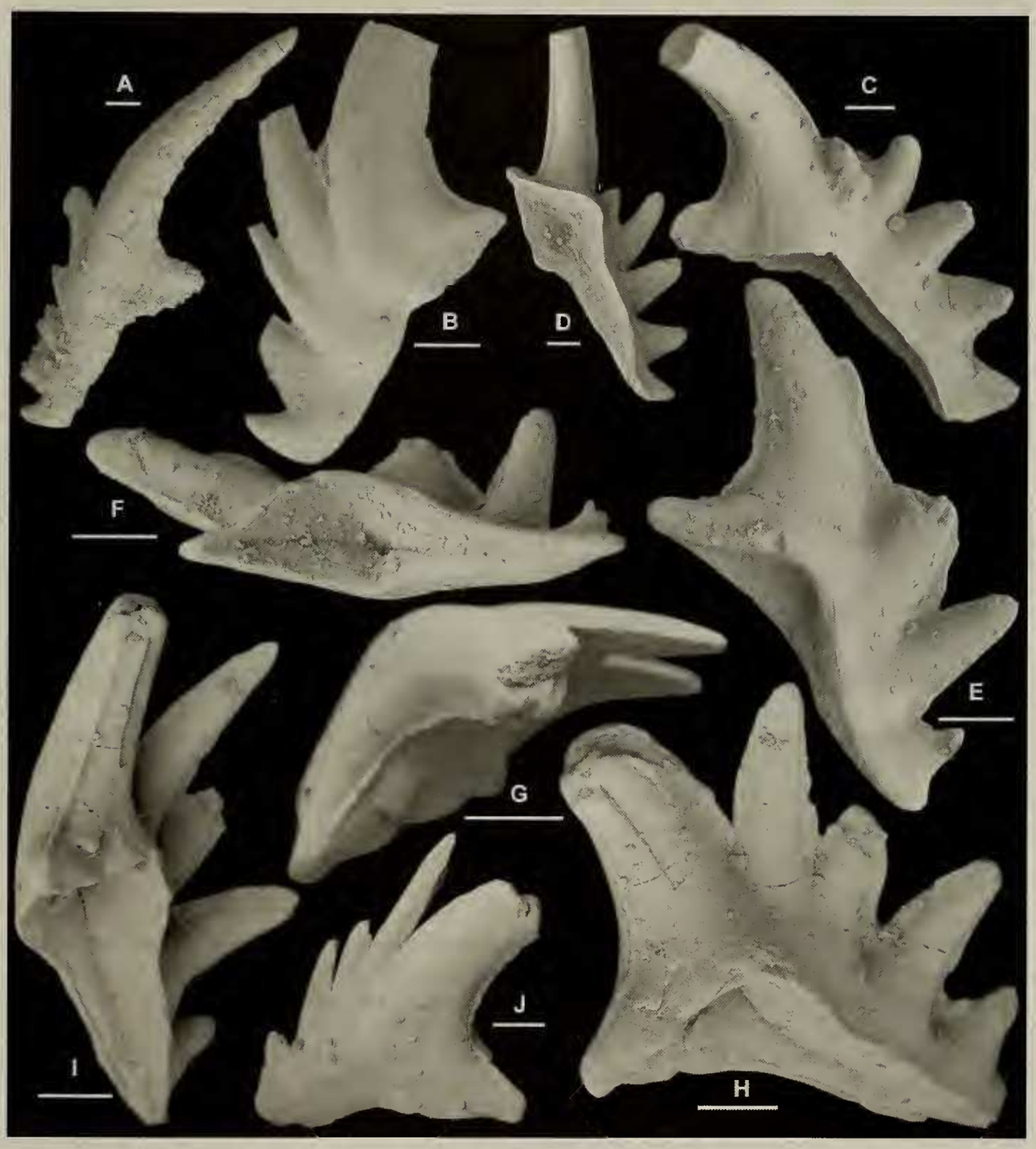

Figure 9. ***Tasmanognathus careyi*** **Burrett, 1979. M element; A, AM F.136527 =UTG96875, JRC 2, anterior view (IY141-025). B, AM F.136528, C137c, anterior view (IY138-011). C-D, AM F.136529, C137c, C, posterior view (IY138-008); D, basal view (IY138-009). E-F, AM F.136530, JRC 2, E, posterior view (IY138-035); F, basal view (IY138-034). G-J, AM F.136531, JRC 2, G, upper view (IY139-007); H, posterior view (IY139-008); I, inner-lateral view (IY139-009); J, anterior view (IY139-010). Scale bars 100 µm.**

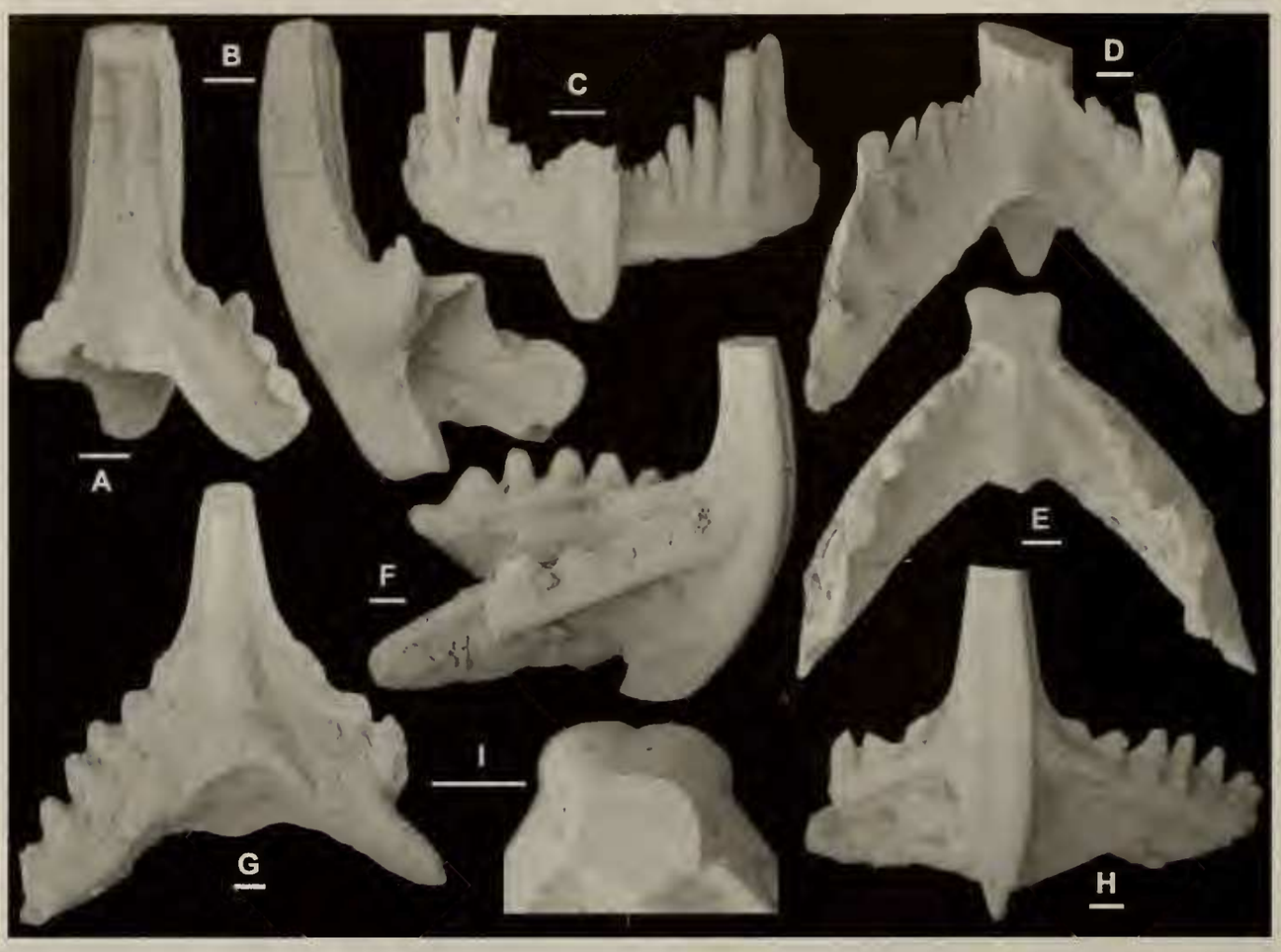

Figure 10. ***Tasmanognathus careyi*** **Burrett, 1979. Sa element; A-B, AM F.136532 =UTG96874 (Burrett 1979, pl. 1, fig. 19), JRC 2, A, posterior view (IY141-022), B, lateral view (IY141-021); C-E, AM F.136533, YYF5, C, anterior view (IY140-004), D, posterior view (IY140-003), E, upper-posterior view (IY140-001); F-I, AM F.136534, YYF4, F, lateral view (IY135-019), G, posterior view (IY135-020), H, anterior view (IY135-018), I, upper view, close up showing the cross section of the cusp (IY135-022). Scale bars 100 µm.**

UTG 96877, previously designated as a syntype (Burrett 1979, pl. 1, fig. 20) is excluded from this species and re-assigned to *T.* sp. cf. *careyi* representing the Sb position (AM F.136567, Fig. 16G herein). Another previously designated syntype UTG 96872 (Burrett 1979, pl. 1, fig. 12) is also excluded from this species and re-assigned to *Chirognathus tricostatus* sp. nov. where it represents the Sb position (AM F.136494, Fig. 4G-H herein).

Diagnosis

Septimembrate apparatus with a ramiform-pectiniform structure including makellate M, alate Sa, digyrate Sb, bipennate Sc, tertiopedate Sd, carminate Pa, angulate Pb1, and pastinate Pb2 elements. S elements with a robust cusp, an open and shallow basal cavity, and long closely-spaced denticles on the processes; Pa element with a longer anterior process, a nearly straight basal margin and a cusp varying from prominently larger (juvenile) than adjacent denticles to rather indistinctive in size (when mature). Pb1 element with a robust cusp, and a strongly curved basal margin. Pb2 element with a short adenticulate outer lateral process, long denticulate anterior and posterior processes, and a strongly laterally flared base.

Description

M element makellate with a denticulate inner-lateral process bearing three to five pointed denticles (Fig. 9), and a shorter, typically adenticulate outer lateral process (Fig. 9A-C, H); cusp robust, antero-posteriorly compressed (Fig. 9G), with a sharp costa along the inner-lateral and outer lateral margins (Fig. 9G-I), and distally curved posteriorly (Fig. 9C-D, G); denticles on the inner lateral process also antero-

Figure 11. ***Tasmanognathus careyi*** **Burrett, 1979. Sb element; A, AM F.136535 =UTG96873, posterior view (IY141-027); B-D, AM F.136536, C98, B, basal view (IY137-039), C, anterior view (IY137-037), D, basal-posterior view (IY137-038); E, AM F.136537, C98, outer-anterior view (IY137-034); F-H, AM F.136538 =UTG96898 (Burrett, 1979, fig. 4A), C98, F, anterior view (IY137-031), G, upper view (IY137-032), H, upper-posterior view (IY137-030). Scale bars 100 μm.**

posteriorly compressed, with a sharp costa along the inner-lateral and outer-lateral margins (Fig. 9C, G-H); basal cavity shallow and open, tapering towards distal ends of the processes and flaring posteriorly (Fig. 9D, F), and often with weakly developed zone of recessive basal margins (Fig. 9F); anterior portion of basal margin nearly straight (Fig. 9B, J), but posterior portion weakly curved (Fig. 9C, E, H).

Sa element alate (Fig. 10), symmetrical with a robust cusp, a prominent tongue-like anticusp, and a long denticulate lateral process on each side; cusp proclined, subquadrate in cross section (Fig. 10E, I), with a sharp costa on each side (Fig. 10A-B) and often a weak costa along the posterior margin (Fig. 10D-E), but some specimens with a broad posterior face (Fig. 10G) or with a broad carina developed (Fig. 10A); broad anterior face bearing a shallow but prominent mid groove and a broad carina on each side (Fig. 10C, H); cusp extended downward to form a downward extending tongue-like anticusp (Fig. 10A-D, H); lateral process long, bearing up to ten or more closely spaced denticles (Fig. 10C-D, H), which are compressed antero-posteriorly; basal cavity open and shallow, flared posteriorly; basal margin arched in posterior view (Fig. 10D).

Sb element digyrate, asymmetrical, with a robust cusp, long denticulate process on each side, and a prominent downwardly extending tongue-like anticusp (Fig. 11); cusp suberect, slightly curved inward (Fig. 10A), with a more strongly convex anterior face, and a sharp costa on each side (Fig. 11G-H); outer lateral process shorter, bearing three or more denticles (Fig. 11A, D, G); inner lateral process longer, bearing five or more peg-like denticles (Fig. 11C, F), and more strongly curved posteriorly (Fig. 11B, G), forming an angle of about 100-110 degrees between the two processes in the upper or basal view (Fig. 11B, G).

Sc element bipennate, asymmetrical with a robust cusp, a long denticulate posterior process, and a short denticulate anterior process (Fig. 12); cusp suberect basally and reclined distally (Fig. 12A, F, H) with a more convex outer lateral face, and laterally compressed with a sharp costa forming anterior

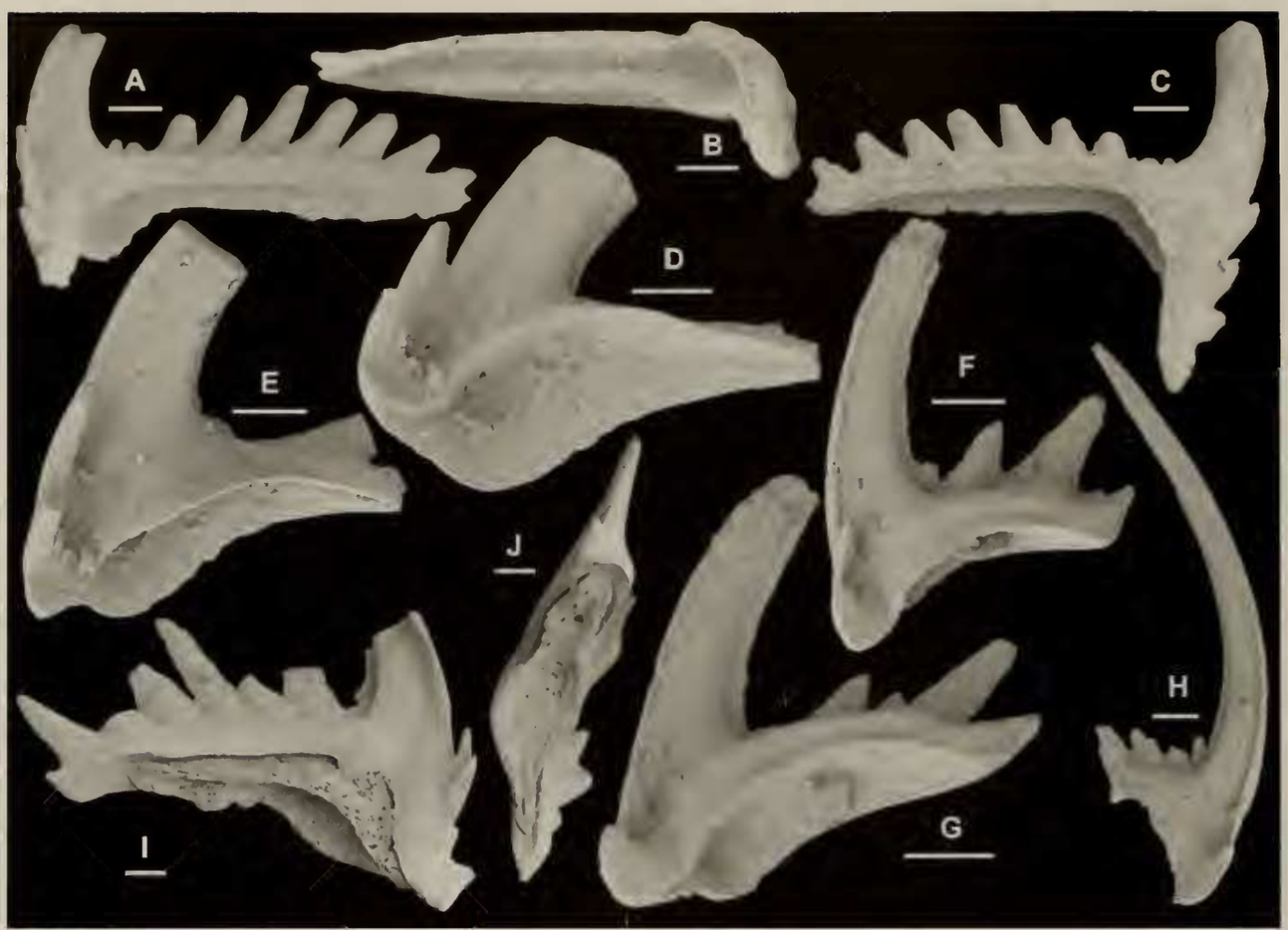

Figure 12. ***Tasmanognathus careyi*** **Burrett, 1979. Sc element; A-C, AM F.136539 =UTG96876 (Burrett 1979, pl. 1, fig. 11), JRC 2, paralectotype, A, inner lateral view (IY141-020), B, basal view (IY141-016), C, outer lateral view (IY141-015); D-E, AM F.136540, YYF5, D, inner-basal view (IY135-041); E, inner-lateral view (IY135-040); F-G, AM F.136541, JRC 2, F, inner lateral view (IY139-028); G, inner-basal view (IY139-027); H, AM F.136542, YYF5, inner-lateral view (IY140-009); I-J, AM F.136543 =UTG 96899 (Burrett, 1979, fig. 4B), C98, 1, inner-lateral view (IY137-029), J, basal view (IY137-027). Scale bars 100 µm.**

and posterior margins (Fig. 12F-I); anterior margin curved inward (Fig. 12D-I); posterior process bearing three or more (up to seven) denticles, which are laterally compressed and posteriorly reclined (Fig. 11A, C, I); anterior process with upper margin curved inwards, and extending downwards bearing two to four small denticles (Fig. 12D-H); basal cavity open and shallow, slightly flared inwards (Fig. 12B, D, G), some specimens with basal funnel attached (Fig. 12I-J).

Sd element tertiopedate, weakly asymmetrical to nearly symmetrical with a robust cusp, a prominent anticusp, a denticulate posterior process and a denticulate lateral process on each side (Fig. 13); cusp with a broad anterior face (Fig. 13B-C), and with a prominent costa along the posterior margin and on each lateral side (Fig. 13D, G); anticup short and downward extending (Fig. 13C-D); posterior process long and straight, broken in most specimens, in one of the examined specimens bearing ten denticles (Fig. 13A); lateral process bearing four or more denticles (Fig. 13B-D); basal cavity open, T-shaped in basal view (Fig. 13B).

Pa element carminate (Fig. 14), laterally compressed and blade-like, with a small cusp, and with the anterior and posterior processes bearing basally confluent denticles; cusp erect (smaller specimens, Fig. 14C, E) to slightly inclined (larger specimens, Fig. 14A, D), typically larger and higher than adjacent denticles (Fig. 14C, E, F), but less distinctive in the larger specimens (Fig. 14 A, H); two processes of unequal length, anterior process longer and higher, bearing five to eight closely-spaced denticles; posterior process lower and shorter, bearing two to six denticles, with distal end slightly bent downward (Fig. 14A, D); juvenile specimens

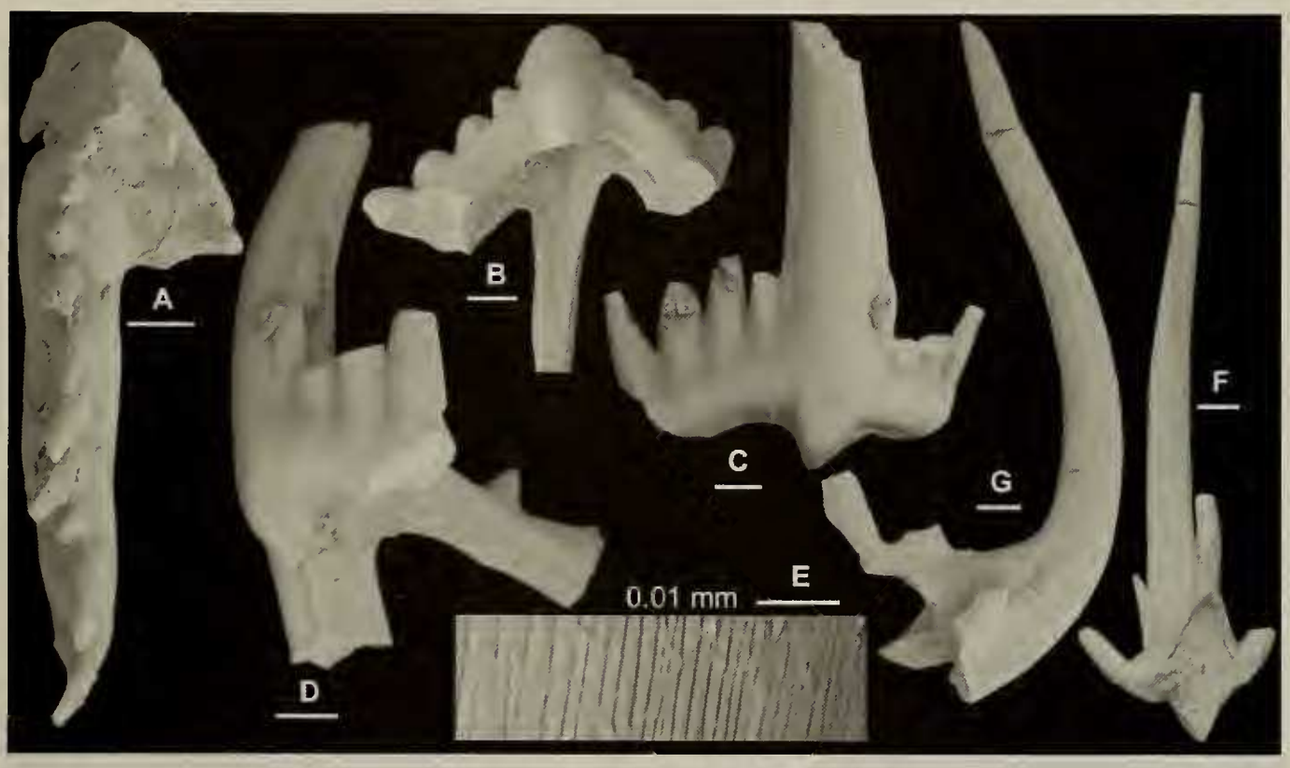

Figure 13. *Tasmanognathus careyi* **Burrett, 1979. Sd element; A, AM F.136544 =UTG96902 (Burrett, 1979, pl. 1, figs 15-16), LLMB, upper view (IY137-033); B-E, AM F.136545 =UTG96900 (Burrett, 1979, fig. 4C-D), B, basal view (IY137-023), C, anterior view (IY137-022), D, lateral view (IY127-024), E, close up showing fine striae on the surface of the cusp (IY137-026); F-G, AM F.136546, YYF1, G, lateral view (IY140-015), F, basal-posterior view (IY140-014). Scale bars 100 μm.**

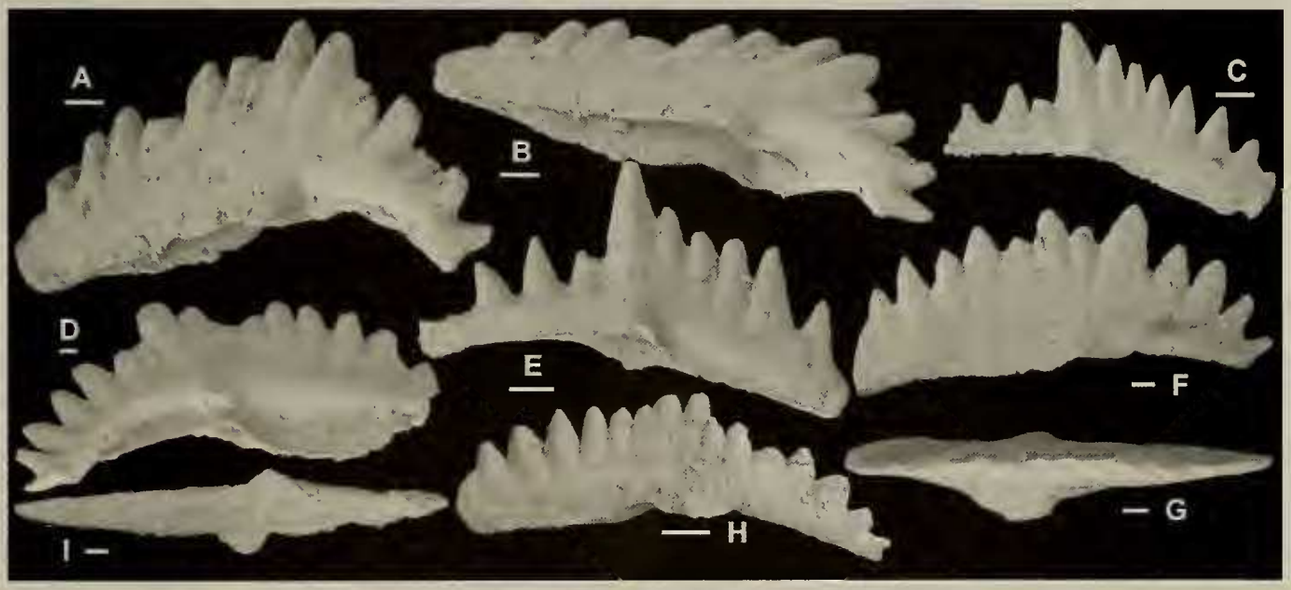

Figure 14. *Tasmanognathus careyi* **Burrett, 1979. Pa element; A-B, AM F.136547 =UTG96851 (Burrett 1979, pl. 1, fig. 6), lectotype, JRC 2, A, outer lateral view (IY141-002), B, basal-inner lateral view (IY141-003); C, AM F.136548 =UTG96856 (Burrett 1979, pl. 1, fig. 7), paralectotype, JRC 2, outer lateral view (IY141-004); D, AM F.136549 =UTG96893a (Burrett, 1979, fig. 3), LLM (B), inner-lateral view (IY137-001); E, AM F.136550 =UTG96893b (Burrett, 1979, fig. 3), LLM (B), outer-lateral view (IY137-003); F-G, AM F.136551, C98, F, outer-lateral view (IY137-005), G, upper view (IY137-006); H-I, AM F.136552, JRC 2, H, inner-lateral view (IY137-010), I, basal view (IY137-009). Scale bars 100 μm.**

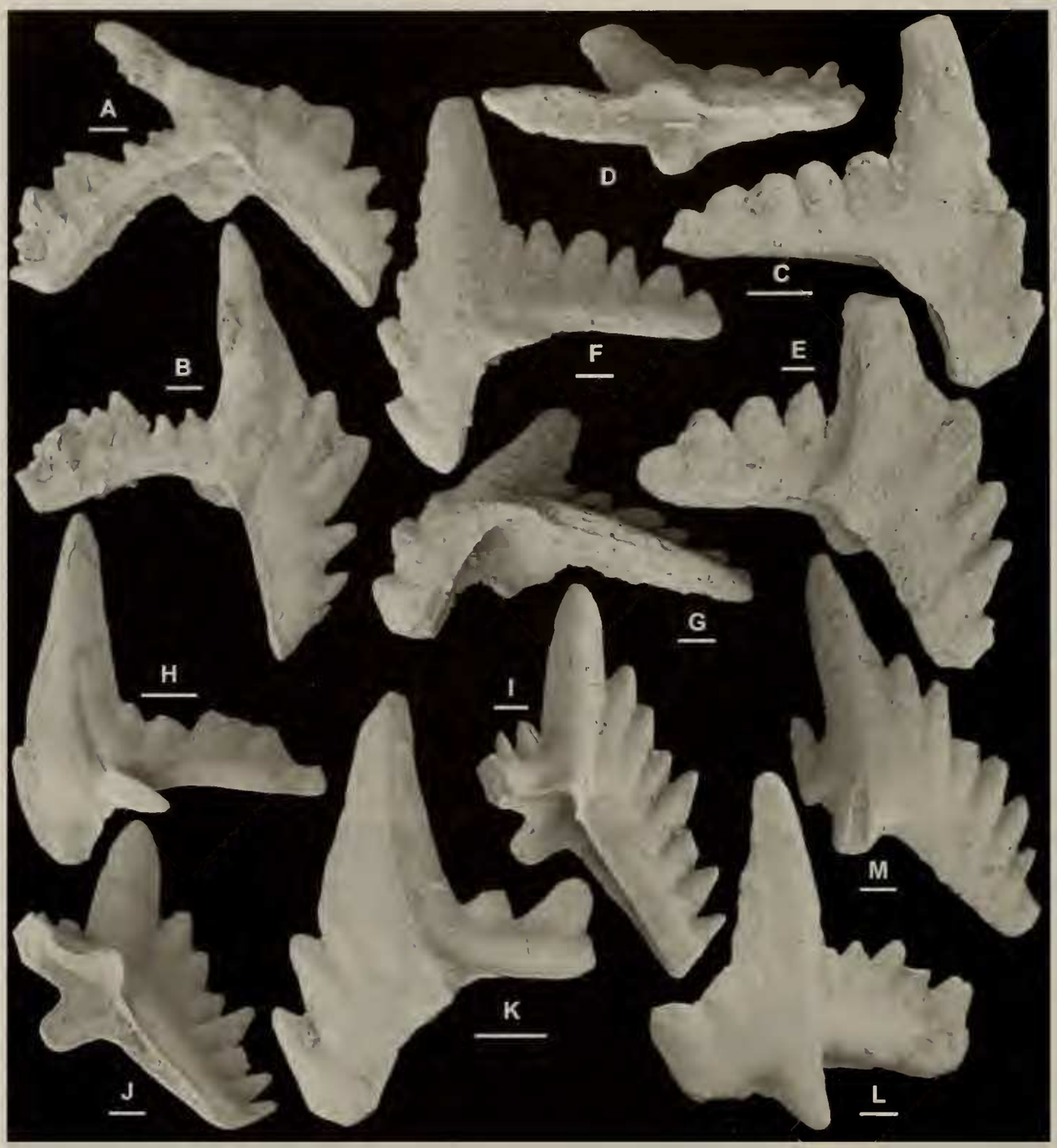

Figure 15. *Tasmanognathus careyi* **Burrett, 1979. A-G, Pb1 element; A-B, AM F.136553 =UTG96850 (Burrett 1979, pl. 1, fig. 4), paralectytype, JRC 2, A, basal-outer lateral view (IY141-007), B, outer lateral view (IY141-006); C, AM F.136554 =UTG96882 (Burrett 1979, pl. 1, fig. 5), paralectotype, JRC 2, inner lateral view (IY141-008); D-E, AM F.136555, C98, D, basal view (IY137-018), E, inner lateral view (IY137-019); F-G, AM F.136556, C98, F, outer-lateral view (IY137-021), G, basal view (IY137-020). H-M, Pb2 element; H, AM F.136557 =UTG96857 (Burrett 1979, pl. 1, fig. 1), paralectotype, JRC 2, outer lateral view (IY141-009); I-J, AM F.136558, JRC 2, I, inner-lateral view (IY137-040), J, basal view (IY137-041); K, AM F.136559 =UTG96860 (Burrett 1979, pl. 1, fig. 2), paralectotype, JRC 2, outer lateral view (IY141-011); L, AM F.136560 =UTG96853 (Burrett 1979, pl. 1, fig. 3), paralectotype, JRC 2, outer lateral view (IY141-012); M, AM F.136561, JRC 2, outer-lateral view (IY137-014). Scale bars 100 µm.**

exhibiting a prominently lower and shorter posterior process with two to four less closely-spaced denticles (Fig. 14C, E); basal cavity shallow and open, flared laterally and extended toward distal end of the processes as a tapering shallow groove (Fig. 14I); basal margin nearly straight to slightly arched in lateral view (Fig. 14A, C-E, F).

Pb1 element angulate (Fig. 15A-G), laterally compressed and blade-like, with a robust cusp, and denticulate anterior and posterior processes; cusp strongly compressed laterally, more convex outer laterally, suberect and slightly curved inwards with sharp anterior and posterior margins; two processes typically sub-equal in length (Fig. 15E) or with slightly longer posterior process (Fig. 15B, C), bearing three to six short, laterally compressed and basally confluent denticles; anterior process extending downward forming an angle of about 100-120 degrees between the two processes in lateral view (Fig. 15B, F); basal cavity shallow and open, laterally flared and extended as a shallow groove underneath each process (Fig. 15D, G).

Pb2 element pastinate (likely a variant of the Pb1 element), with a robust cusp, long denticulate anterior and posterior processes, and a short adenticulate outer lateral process (Fig. 15H-M); cusp suberect (Fig. 15H), laterally compressed, with a broad smooth inner lateral face, and sharp anterior and posterior margins, outer lateral face smooth (Fig. 15L-M) or with a mid costa (Fig. 15H, K); anterior process typically longer, bearing up to seven or more denticles, which are typically closely spaced with confluent bases (Fig. 15I, M); most specimens with posterior process broken, bearing up to five denticles (Fig. 15L); outer lateral process typically represented by a prominent tongue-like basal extension (Fig. 15J-M), or as a short adenticulate process (Fig. 15H); basal cavity shallow, outer laterally flared more strongly, and tapering as a shallow groove to the distal end of anterior and posterior processes (Fig. 15I-J).

Discussion

One originally designated syntype (AM F.136567 =UTG96877 Fig. 16G; also see Burrett 1979, pl. 1, fig. 20) and an additional figured specimen (AM F.136562 =UTG96904, Fig. 16A; also see Burrett 1979, pl. 1, figs 8-10) of *T. careyi* are excluded from this species and re-assigned to represent the Sb and Pb2 elements of *T.* sp. cf. *careyi*, as they exhibit more widely spaced denticles on the processes.

The original definition of the S element given by Burrett (1979) is more or less followed herein, except that his Sa1 element (Burrett 1979, fig. 4C-D) is now assigned to the Sd position (Fig. 13), the digyrate element with a longer inner lateral process (Burrett 1979, fig. 4A, referred to as Sc) to the Sb position (Fig. 11), and the bipennate element with a shorter downwardly extended and inner laterally curved anterior process (Burrett 1979, fig. 4B, referred to as Sb) to the Sc position (Fig. 12). Burrett (1978, p. 34) further recognized an Sa2 element with the cusp exhibiting a subquadrate cross section, but illustrated it as Sa (Burrett 1979, pl. 1, fig. 19; also Fig. 10A-B herein). This symmetrical or nearly symmetrical element (Fig. 10) is confirmed as occupying the Sa position. The makellate M element (Fig. 9) described herein was not recognized in Burrett's original description of *T. careyi*. Specimens originally included in the Pa element by Burrett (1979) show two morphotypes, which are defined herein to represent the Pb1 (Burrett 1979, pl. 1, figs 4-5; Fig. 15A-G) and Pb2 (Burrett 1979, pl. 1, figs 1-3; Fig. 15H-M) elements. They can be easily differentiated from each other by having a short tongue-like outer lateral process, a costa on the outer lateral face or a short adenticulate outer lateral process in the Pb2 element (Fig. 15H-M).

Burrett (1979, pp. 33-34) discussed the considerable ontogenetic variations among the P elements, in particular the posterior process of the Pa element (referred to as the Pb element by Burrett, 1979, see p. 33, fig. 3) and the anterior process of the Pb2 element (assigned to part of the Pa element by Burrett, 1979, see p. 33, fig. 2). Juveniles of the Pa element have a larger cusp and a lower posterior process with less closely spaced denticles (Fig. 14C, E; Burrett 1979, fig. 3). It cannot presently be established whether the distinctions between the Pb1 and Pb2 elements, and within the Pa elements, represent ecophenotypic variations, or whether they reflect a high degree of morphological plasticity.

T. careyi has been widely reported from North China (Zhao et al. 1984; Wang and Luo 1984; Pei and Cai 1987; An and Zheng 1990). However, judging from the illustrations of these specimens, none can be confidently assigned to the Tasmanian species, except for one specimen figured by An and Zheng (pl. 11, fig. 2) from the lower part of the Yaoxian Formation in the Ordos Basin of Shaanxi Province that is comparable with the Pa element of *T. careyi*. Pa elements of *T. borealis* (An in An et al. 1985, pl. 1, fig. 14) and *T. multidentatus* (An and Zheng 1990, pl. 11, fig. 4; = *T. borealis*), also from the Yaoxian Formation of the Ordos Basin, similarly have an indistinct cusp that is nearly the same size as adjacent denticles, but the outline of these two illustrated specimens is shorter and higher in comparison with the Pa element of *T. careyi* (Fig. 14).

Figure 16. Tasmanognathus sp. cf. careyi Burrett, 1979. A, Pb2 element, AM F.136562 =UTG96904 (Burrett, 1979, pl. 1, figs 8-10), LLM (B), outer-lateral view (IY137-007). B, M element, AM F.136563, YYF1, posterior view (IY136-032). C-F, Sa element; C-D, AM F.136564, JRC 2, C, Posterior view (IY138-006); D, postero-basal view (IY138-005); E, AM F.136565, JRC 2, posterior view (IY139-029); F, AM F.136566, YYF1, anterior view (IY140-010). G, Sb element, AM F.136567 =UTG96877 (syntype of T. careyi; Burrett 1979, pl. 1, fig. 20), JRC 2, posterior view (IY141-024). H-I, Sd element, AM F.136568, YYF4, H, posterior view (IY135-023), I, upper view (IY135-024); J-K, Sc element, AM F.136569, YYF1, J, inner lateral view (IY140-013), K, outer lateral view (IY140-012). Scale bars 100 μm.

Tasmanognathus sp. cf. *T. careyi* Burrett, 1979
Figures 16-17

Synonymy

Tasmanognathus careyi Burrett, 1979, p. 33-35, *partim* only pl. 1, figs 8-10 (= Pb2 element), fig. 20 (= Sb element).

Material

34 specimens from four samples in the Settlement Road section of Florentine Valley area (see Table 1).

Diagnosis

A species of *Tasmanognathus* having an septimembrate apparatus, including makellate M, alate Sa, digyrate Sb, bipennate Sc, digyrate? (modified tertiopedate) Sd, carminate Pa, angulate? (bipennate) Pb1, and pastinate Pb2 elements; elements robust and large in size bearing a prominent cusp ornamented with fine striae, and small widely spaced denticles on the processes of M, S, Pb1 and Pb2 elements; most elements with basal funnel attached.

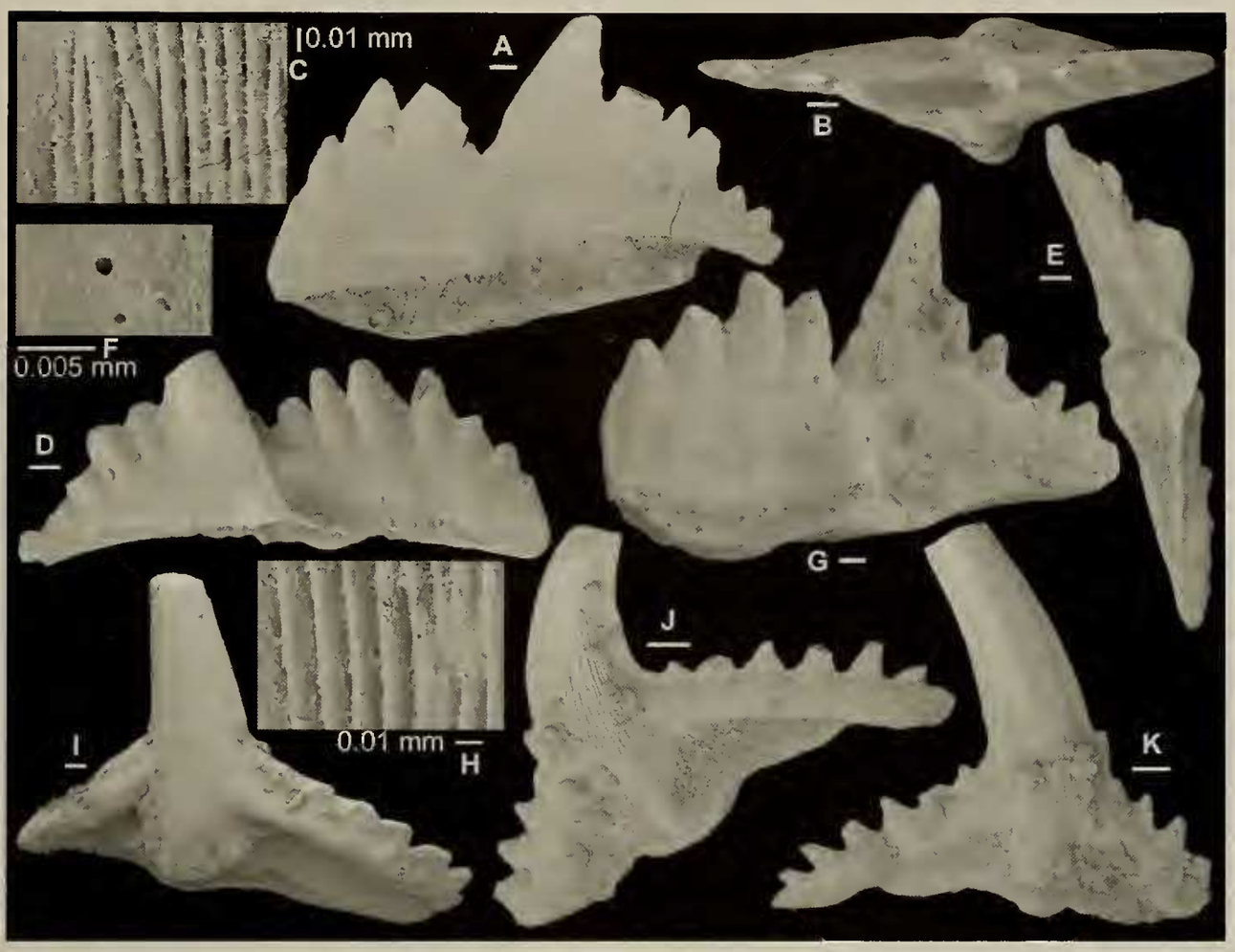

Fig. 17. ***Tasmanognathus*** **sp. cf.** ***T. careyi*** **Burrett, 1979. A-H, Pa element; A-C, AM F.136570, YYF4, A, inner-lateral view (IY135-005), B, upper view (IY135-003), C, outer-lateral view, close up showing fine surface striae (IY135-007); D-F, AM F.136571, YYF4, D, outer-lateral view (IY135-009), E, basal view (IY135-008), F, outer-lateral view, close up showing rounded boring hole on the surface (IY135-010); G-H, AM F.136572, YYF4, G, inner lateral view (IY140-037), H, close up showing fine surface striae (IY140-038). I-K, Pb1 element; I, AM F.136573, YYF4, outer-lateral view (IY135-012); J-K, AM F.136574, YYF4, J, inner-lateral view (IY140-031), K, outer lateral view (IY140-030). Scale bars 100 µm unless otherwise indicated**

Description

M element with a long, denticulate inner-lateral process bearing five short and widely spaced denticles (Fig. 16B), and a short, outer lateral process bearing two small rudimentary denticles; cusp robust, antero-posteriorly compressed with a sharp costa along the inner-lateral and outer lateral margins and distally curved posteriorly.

Sa element alate (Fig. 16C-F), with a robust cusp and a long denticulate lateral process on each side; cusp strongly compressed antero-posteriorly, with a sharp costa along the lateral margins; lateral process long, bearing three or more peg-like denticles (Fig. 16C), which are also strongly compressed antero-posteriorly, basal cavity open and shallow, flared posteriorly, isosceles-triangular in basal view (Fig. 16D-E); basal margin gently arched in posterior view (Fig. 16C).

Sb element digyrate, like Sa but asymmetrical (Fig. 16G); cusp robust and antero-posteriorly compressed with sharp lateral margins; denticulate lateral process on each side bearing two or three short widely-spaced denticles; inner lateral process longer and more downwardly extending.

Sc element bipennate, strongly asymmetrical with a robust cusp, denticulate anterior and posterior processes (Fig. 16J-K); cusp distally curved inner laterally with a more convex outer lateral face bearing a prominent costa; posterior process longer and slightly arched bearing three widely-spaced denticles; anterior process curved inward bearing two widely-spaced denticles.

Sd element digyrate? with a robust cusp, a long denticulate lateral process on each side, a sharp costa on the posterior face and a broad anterior face with a weak carina (Fig. 16H-I); cusp with a sharp costa on each side and on the posterior face, and ornamented with fine striae; inner lateral process longer bearing eight small denticles.

Pa element blade-like with a prominent cusp, and denticulate anterior and posterior processes (Fig. 17A-H); cusp suberect or slightly inclined posteriorly, laterally compressed, standing higher above the adjacent denticles, and about twice width of the adjacent denticles on the anterior process, and typically leaving a prominent notch between cusp and the first denticle on the anterior process (Fig. 17A, G); anterior process higher and longer bearing four to eight larger and basally confluent denticles (Fig. 17A, D, G); posterior process slightly shorter, triangular in outline in lateral view, with a tapering distal end and bearing five or six smaller denticles (Fig. 17A, G); basal cavity shallow, flared laterally, forming a shallow groove underneath each process (Fig. 17E), and with a straight basal margin (Fig. 17D); some specimens bearing fine rounded boring holes (Fig. 17F).

Pb1 element asymmetrical with a suberect, robust cusp and long denticulate anterior and posterior processes (Fig. 17I-K); cusp curved inward, diamond-shaped in cross section with a sharp costa along the anterior and posterior margins, a mid costa on the inner lateral face (Fig. 17J), and a broad carina on the outer lateral face (Fig. 17K); two processes bearing small, discrete denticles; posterior process longer with six or more denticles, and anterior process shorter, extending downwards (Fig. 17K).

Pb2 element pastinate, with a robust cusp and denticulate anterior, posterior and outer lateral processes (Fig. 16A); cusp laterally compressed with a sharp costa along anterior and posterior margins and on the outer lateral face; long anterior and posterior processes bearing short, widely spaced denticles; outer lateral process short, represented by a single denticle.

Discussion

This species differs from *T. careyi* in having a Pa element with shorter and higher outline bearing a prominent cusp and a notch in front of the cusp, and in having the S, Pb1 and Pb2 elements bearing small, discrete or widely-spaced denticles on the processes. Additional specimens from the Settlement Road section of Florentine Valley area confirm that it represents a separate species of *Tasmanognathus*. However, as only a small number of specimens are available for study, this species is retained herein under open nomenclature pending further collecting and study.

ACKNOWLEDGMENTS

Field work in Tasmania by Zhen was supported by a grant from the Betty Mayne Scientific Research Fund of the Linnean Society of New South Wales. Burrett's study was funded by the Australian Research Council. Gary Dargan (Geological Survey of New South Wales) assisted with acid leaching and residue separation. Scanning electron microscope photographs were prepared in the Electron Microscope Unit of the Australian Museum. We thank Stephen Leslie and John Pickett for their perceptive and constructive reviews of the manuscript. The study was undertaken by Zhen as part of a CAS/SAFEA International Partnership Program for Creative Research Teams, and is a contribution to IGCP Project 503: Ordovician Palaeogeography and Palaeoclimate. Percival publishes with permission of the Director of the Geological Survey of New South Wales.

REFERENCES

Aldridge, R.J. and Smith, M.P. (1993). Conodonta. 563-572. In Benton, M.J. (ed.), 'The Fossil Record 2'. 845 p. (Chapman and Hall, London).

An, T.X., Zhang, F., Xiang, W.D., Zhang, Y.Q., Xu, W.H., Zhang, H.J., Jiang, D.B., Yang, C.S., Lin, L.D., Cui, Z.T. and Yang, X.C. (1983). 'The conodonts in North China and adjacent regions'. 223 p. (Science Press: Beijing) (in Chinese with English abstract).

An, T.X., Zhang, A.T. and Xu, J.M. (1985). Ordovician conodonts from Yaoxian and Fuping, Shaanxi Province, and their stratigraphic significance. *Acta Geologica Sinica* **59**, 97-108 (in Chinese with English abstract).

An, T.X. and Zheng, S.C. (1990). 'The conodonts of the marginal areas around the Ordos Basin, North China'. 199 pp. (Science Press: Beijing) (in Chinese with English abstract).

Banks, M.R. and Burrett, C.F. (1980). A preliminary Ordovician biostratigraphy of Tasmania. *Journal of the Geological Society of Australia* **26**, 363-375.

Balfour, F. M. (1880–1881). A treatise on comparative embryology. Two volumes. Macmillan & Co., London.

Bergström, S.M. and Sweet, W.C. (1966). Conodonts from the Lexington Limestone (Middle Ordovician) of Kentucky and its lateral equivalents in Ohio and Indiana. *Bulletin of American Paleontology* **50 (229)**, 271-441.

Branson, E.B. and Mehl, M.G. (1933). Conodont studies. *University of Missouri Studies* **8**, 1-349.

Burrett, C.F. (1978). Middle–Upper Ordovician conodonts and stratigraphy of the Gordon Limestone Sub-group, Tasmania. Unpublished PhD thesis, University of Tasmania, 342p.

Burrett, C.F. (1979). *Tasmanognathus*: a new Ordovician conodontophorid genus from Tasmania. *Geologica et Palaeontologica* **13**, 31-38.

Burrett, C.F., Banks, M.R., Clota, G. and Seymour, D. (1989). Lithostratigraphy of the Ordovician Gordon Group, Mole Creek, Tasmania. *Records of the Queen Victoria Museum, Launceston* **96**, 1-14.

Burrett, C.F., Long, J. and Stait, B. (1990). Early-Middle Palaeozoic biogeography of Asian terranes derived from Gondwana. In 'Palaeozoic Palaeogeography and Biogeography' (eds McKerrow, W.S. and Scotese, C. R.). *Geological Society Memoir* **12**, 163-174.

Burrett, C.F., Stait, B.A., and Laurie, J. (1983). Trilobites and microfossils from the Middle Ordovician of Surprise Bay, southern Tasmania, Australia. *Memoir of the Australian Association of Palaeontologists* **1**, 177-193.

Burrett, C.F., Stait, B.A., Sharples, C. and Laurie, J. (1984). Middle-Upper Ordovician shallow platform to deep basin transect, southern Tasmania, Australia. In 'Aspects of the Ordovician System' (ed D.L. Bruton) Universitetsforlaget, Oslo, 149-158.

Cantrill, R.C. and Burrett, C.F. (2004). The greater Gondwana distribution of the Ordovician conodont *Panderodus nogamii* (Lee) 1975. *Courier Forschungsinstitut Senckenberg* **245**, 407-419.

Chen, X., Rong, J.Y., Wang, X.F., Wang, Z.H., Zhang, Y.D. and Zhan, R.B. (1995). Correlation of the Ordovician rocks of China: charts and explanatory notes. *International Union of Geological Sciences, Publication* **31**, 1–104.

Corbett, K.D. and Banks, M.R. (1974). Ordovician stratigraphy of the Florentine Synclinorium south west Tasmania. *Papers and Proceedings of the Royal Society of Tasmania* **107**, 207-238.

Domoulin, A. G., Harris, A. G., Gagiev, M., Bradley, D. C. and Repetski, J.E. (2002). Lithostratigraphic, conodont, and other faunal links between lower Paleozoic strata in northern and central Alaska and northeastern Russia. *Geological Society of America, Special Paper* **360**, 291-312.

Ethington, R.L. (1959). Conodonts of the Ordovician Galena Formation. *Journal of Paleontology* **33**, 257-292.

Goodwin, P.W. and Anderson, E.J. (1985). Punctuated Aggradational Cycles: a general hypothesis of episodic stratigraphic accumulation. *Journal of Geology* **93**, 515-533.

Jing, X.C., Yang, Z.L., Zhang, F., Zhang, S.B. and Deng, S.H. (2007). Conodont biostratigraphy of Ordovician outcrop section in Kalpin region of the Tarim Basin, Xinjiang, China. *Acta Palaeontologica Sinica* **46** (Suppl.), 201-207.

Laurie, J.R. (1991). Articulate brachiopods from the Ordovician and Lower Silurian of Tasmania. *Memoir of the Australian Association of Palaeontologists* **11**, 1-106.

Lee, H.Y. (1975). Conodonten aus dem unteren und mittleren Ordovizium von Nordkorea. *Palaeontographica Abteilung* A **150**, 161-186.

Lee H. Y. (1982). Conodonts from the Hoedongri Formation (Silurian), western Jeongseon area, Kangweon-do, South Korea. *Journal of the National Academy of Sciences, Republic of Korea, Natural Sciences* **21**, 43-131.

Leslie, S.A. (1997). Apparatus architecture of *Belodina* (Conodonta): Interpretations based on fused clusters of *Belodina compressa* (Branson and Mehl, 1933) from the Middle Ordovician (Turinian) Plattin Limestone of Missouri and Iowa. *Journal of Paleontology* **71**, 921-926.

Leslie, S.A. (2000). Mohawkian (Upper Ordovician) conodonts of eastern North America and Baltoscandia. *Journal of Paleontology* **74 (6)**, 1122-1147.

Leslie, S.A. and Bergström, S.M. (1995). Element morphology and taxonomic relationships of the Ordovician conodonts *Phragmodus primus* Branson and Mehl, 1933, the type species of *Phragmodus* Branson and Mehl, 1933, and *Phragmodus undatus* Branson and Mehl, 1033. *Journal of Paleontology* **69 (5)**, 967-974.

Lin Baoyu and Qiu Hongrong (1990). Geological and geographical distribution of the Ordovician conodont genus *Tasmanognathus* Burrett in North China. *Courier Forschungsinstitut Senckenberg (CFS)* **117**, 55-59.

Lindström, M. (1955). Conodonts from the lowermost Ordovician strata of south-central Sweden. *Geologiska Foreningens i Stockholm Foerhandlinger* **76**, 517-604.

Lindström, M. (1971). Lower Ordovician conodonts of Europe. In 'Symposium on conodont biostratigraphy' (eds W.C. Sweet and S.M. Bergström). *Geological Society of America, Memoir* **127**, 21-61.

Pander, C. H. (1856). 'Monographie der fossilen Fische des Silurischen Systems der Russisch-Baltischen Gouvernements'. 91 p. (Akademie der Wissenschaften, St. Petersburg).

Pei, F. and Cai, S.H. (1987). 'Ordovician conodonts from Henan Province'. 128 p. (Press of the Wuhan College of Geosciences, Wuhan). (in Chinese)

Percival, I.G., Morgan, E.J. and Scott, M.M. (1999). Ordovician stratigraphy of the northern Molong Volcanic Belt: new facts and figures. *Geological Survey of New South Wales, Quarterly Notes* **108**, 8-27.

Percival, I.G., Zhen, Y.Y. and Pickett, J.W. (2006). Late Ordovician faunas from the Quandialla-Marsden district, south-central New South Wales. *Proceedings of the Linnean Society of New South Wales* **127**, 235-255.

Pyle, L.J. and Barnes, C.R. (2002). 'Taxonomy, evolution, and biostratigraphy of conodonts from the Kechika Formation, Skoki Formation, and Road River Group (Upper Cambrian to Lower Silurian), Northeastern British Columbia'. 227 p. (NRC Research Press, Ottawa).

Savage, N.M. (1990). Conodonts of Caradocian (Late Ordovician) age from the Cliefden Caves Limestone,

southeastern Australia. *Journal of Paleontology* **64**, 821-831.

Schopf, T.J. (1966). Conodonts of the Trenton Group (Ordovician) in New York, southern Ontario, and Quebec. *New York State Museum and Science Service Bulletin* **405**, 1-105.

Stait, B. (1984). Ordovician nautiloids of Tasmania - Gouldoceratidae fam. nov. (Discosorida). *Proceedings of the Royal Society of Victoria*, **96 (4)**, 187-207.

Stait, B. (1988). Tasmanian nautiloid faunas – biostratigraphy, biogeography and morphology. *Senckenbergia Lethaia* **69**, 87-107.

Stait, B. and Flower, R.H. (1985). Michelinoceratida (Nautiloidea) from the Ordovician of Tasmania, Australia. *Journal of Paleontology* **59 (1)**, 149-159.

Stauffer, C.R. (1935). Conodonts of the Glenwood beds. *Bulletin of Geological Society of America* **46, 125-168.**

Sweet, W.C. (1982). Conodonts from the Winnipeg Formation (Middle Ordovician) of the northern Black Hills, South Dakota. *Journal of Paleontology* **56**, 1029-1049.

Sweet, W.C. (1988). 'The Conodonta: Morphology, Taxonomy, Paleoecology, and Evolutionary History of a Long-Extinct Animal Phylum'. 212 p. (Clarendon Press, Oxford).

Teichert, C. and Glenister, B.F. (1952). Fossil nautiloid faunas from Australia. *Journal of Paleontology* **26**, 730-752.

Wang X.F., Chen, X., Chen, X.H. and Zhu, C.Y. (1996). 'Stratigraphical Lexicon of China, the Ordovician System'. 126p. (Geological Publishing House, Beijing) (in Chinese).

Wang, Z.H. and Luo, K.Q. (1984). Late Cambrian and Ordovician conodonts from the marginal areas of the Ordos Platform, China. *Bulletin, Nanjing Institute of Geology and Palaeontology, Academia Sinica* **8**, 237-304.

Watson, S.T. (1988). Ordovician conodonts from the Canning Basin (W. Australia). *Palaeontographica Abteilung* A **203 (4-6)**, 91-147.

Webby, B.D., VandenBerg, A.H.M., Cooper, R.A., Banks, M.R., Burrett, C.F., Henderson, R.A., Clarkson, P.D., Hughes, C.P., Laurie, J., Stait, B., Thomson, M.R.A. and Webers, G.F. (1981). The Ordovician System in Australia, New Zealand and Antarctica. Correlation Chart and Explanatory Notes. *International Union of Geological Sciences, Publication No.* **6**, 1-64.

Zhang, J.H., Barnes, C.R. and Cooper, B.J. (2004). Early Late Ordovician conodonts from the Stokes Siltstone, Amadeus Basin, central Australia. *Courier Forschungsinstitut Senckenberg* **245**, 1-37.

Zhao, S.Y., An, T.X., Qiu, H.R., Wan, S.L. and Ding, H. (1984). 'Palaeontological atlas of North China III, Micropalaeontology'. 857 p. (Geological Publishing House, Beijing) (in Chinese).

Zhao, Z.X., Zhang, G.Z. and Xiao, J.N. (2000). 'Paleozoic stratigraphy and conodonts in Xinjiang'. 340 p. (Petroleum Industry Press, Beijing) (in Chinese with English Abstract).

Zhen, Y.Y. and Percival, I.G. (2004a). Middle Ordovician (Darriwilian) conodonts from allochthonous limestones in the Oakdale Formation of central New South Wales, Australia. *Alcheringa*, **28**, 77-111.

Zhen, Y.Y. and Percival, I.G. (2004b). Middle Ordovician (Darriwilian) conodonts from the Weemalla Formation, south of Orange, New South Wales. *Memoirs of the Association of Australasian Palaeontologists*, **30**, 153-178.

Zhen, Y.Y., Percival, I.G. and Farrell, J.R. (2003a). Late Ordovician allochthonous limestones in Late Silurian Barnby Hills Shale, central western New South Wales. *Proceedings of the Linnean Society of New South Wales* **124**, 29-51.

Zhen, Y.Y., Percival, I.G. and Webby, B.D. (2003b). Early Ordovician conodonts from far western New South Wales Australia. *Records of the Australian Museum* **55**, 169-220.

Zhen, Y. Y., Percival, I.G. and Webby, B.D. (2004). Conodont faunas from the Mid to Late Ordovician boundary interval of the Wahringa Limestone Member (Fairbridge Volcanics), central New South Wales. *Proceedings of the Linnean Society of New South Wales* **125**, 141-164.

Zhen, Y.Y. and Webby, B.D. (1995). Upper Ordovician conodonts from the Cliefden Caves Limestone Group, central New South Wales, Australia. *Courier Forschungsinstitut Senckenberg* **182**, 265-305.

Zhen, Y.Y., Webby, B.D. and Barnes, C.R. (1999). Upper Ordovician conodonts from the Bowan Park succession, central New South Wales, Australia. *Geobios* **32**, 73-104.

Ziegler, W. (ed.) (1981). 'Catalogue of Conodonts, Vol. 4'. 445 p. (Schweizerbart'sche Verlagsbuchhandlung, Stuttgart).

Ziegler, W. (ed.) (1991). 'Catalogue of Conodonts, Vol. 5'. 212 p. (Schweizerbart'sche Verlagsbuchhandlung, Stuttgart).